
HyperSHAP: Shapley Values and Interactions for Hyperparameter Importance

Marcel Wever^{1,2} Maximilian Muschalik^{3,4} Fabian Fumagalli⁵ Marius Lindauer^{1,2}

Abstract

Hyperparameter optimization (HPO) is a crucial step in achieving strong predictive performance. However, the impact of individual hyperparameters on model generalization is highly context-dependent, prohibiting a one-size-fits-all solution and requiring opaque automated machine learning (AutoML) systems to find optimal configurations. The black-box nature of most AutoML systems undermines user trust and discourages adoption. To address this, we propose a game-theoretic explainability framework for HPO that is based on Shapley values and interactions. Our approach provides an additive decomposition of a performance measure across hyperparameters, enabling local and global explanations of hyperparameter importance and interactions. The framework, named HYPERSHAP, offers insights into *ablations*, the *tunability* of learning algorithms, and *optimizer behavior* across different hyperparameter spaces. We evaluate HYPERSHAP on various HPO benchmarks by analyzing the interaction structure of the HPO problem. Our results show that while higher-order interactions exist, most performance improvements can be explained by focusing on lower-order representations.

1. Introduction

Hyperparameter optimization (HPO) is an important step in the design process of machine learning (ML) applications to achieve optimal performance for a given dataset and performance measure (Snoek et al., 2014; Bischl et al., 2023). This is particularly true for deep learning, where hyperparameters describe the neural architecture and steer the learning behavior, e.g., via the learning rate (Zimmer et al., 2021). Also, in the age of generative AI and fine-tuning of large foundation models, HPO is key for achieving state-of-

the-art results (Yin et al., 2021; Tribes et al., 2023; Wang et al., 2023).

Hyperparameters affect the generalization performance of models in varied ways, with some having a more significant impact on tuning than others (Bergstra & Bengio, 2012; Hutter et al., 2014; Zimmer et al., 2021). The influence of hyperparameters on generalization performance is highly context-dependent, varying with the dataset characteristics (e.g., size, noise level) and the specific performance measure being optimized (e.g., accuracy, F1 score) (Bergstra & Bengio, 2012; van Rijn & Hutter, 2018). This complexity makes HPO particularly challenging, requiring opaque automated machine learning (AutoML) systems to find optimal configurations within large search spaces (Feurer et al., 2015; Wever et al., 2021). Yet, even after arriving at an optimized hyperparameter configuration, understanding *why it outperforms other configurations* remains difficult due to intricate effects and interactions among hyperparameters.

Despite their promise, AutoML systems have not fully permeated user groups such as domain experts, ML practitioners, and ML researchers (Lee et al., 2019; Bouthillier & Varoquaux, 2020; Hasebrook et al., 2023; Simon et al., 2023). This lack of adoption stems, in part, from the rigidity of many AutoML systems, which are often difficult to adapt to specific use cases, but is also attributed to the lack of transparency and interpretability (Wang et al., 2019; Drozdal et al., 2020). Studies highlight that a concrete requirement often requested by AutoML system users is interpretability (Wang et al., 2019; Xin et al., 2021; Hasebrook et al., 2023; Sun et al., 2023), and its lack has even led users to favor manual development for high-stakes projects (Xin et al., 2021). For ML researchers, explanations of HPO processes are particularly relevant, as they often prioritize understanding the effectiveness of individual ML components and require control over key aspects of model behavior. Similarly, AutoML researchers need such kind of information to analyze AutoML systems' performance and behavior. Prior works on hyperparameter importance analysis (Hutter et al., 2014; Watanabe et al., 2023; Theodorakopoulos et al., 2024) and hyperparameter effects (Moosbauer et al., 2021; Segel et al., 2023) show that addressing these interpretability gaps is critical for building trust and enabling more effective use of AutoML systems in a synergetic way with ML experts and data scientists (Lindauer et al., 2024).

¹L3S Research Center, Germany ²Leibniz University Hannover, Germany ³Munich Center for Machine Learning, Germany ⁴LMU Munich, Germany ⁵Bielefeld University, Germany. Correspondence to: Marcel Wever <m.wever@ai.uni-hannover.de>.

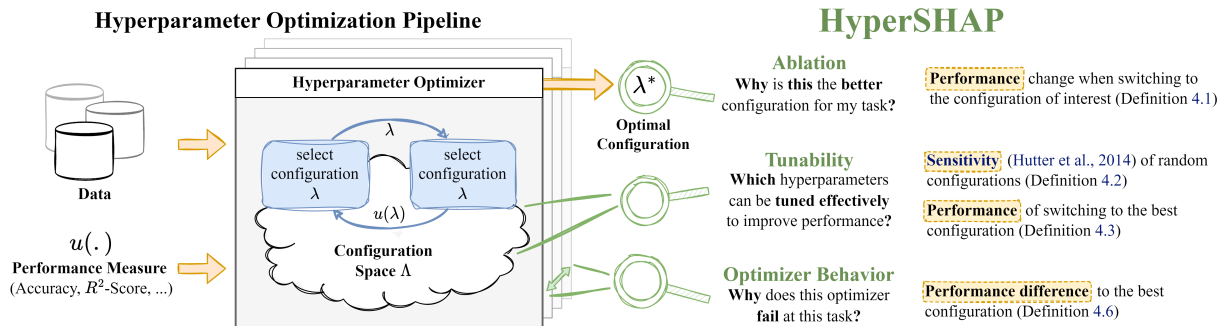


Figure 1. Game-theoretic explanations as defined with HYPERSHAP’s hyperparameter importance games can be used to gain insights into hyperparameter values, hyperparameter configuration spaces, datasets, and different hyperparameter optimizers. HYPERSHAP can be used for data-specific explanations or explanations across datasets.

1.1. Contribution

In this paper, we formalize HYPERSHAP, a post-hoc explanation framework for hyperparameter importance:

- (1) We define a comprehensive set of 5 explanation games and interpret them using the Shapley value and interactions on three levels: specific configurations, hyperparameter spaces, and optimizer bias.
- (2) With HYPERSHAP, we elicit hyperparameter importance and interaction structures for various benchmarks, observing the existence of higher-order interactions.
- (3) We apply HYPERSHAP to various explanation tasks and demonstrate its versatility.

1.2. Related Work

Hyperparameter importance (HPI) has gained significant attention in machine learning due to its crucial role in justifying the need for HPO and in attributing performance improvements to specific hyperparameters (Probst et al., 2019; Pushak & Hoos, 2020; 2022; Schneider et al., 2022). A variety of approaches have been developed to assess how different hyperparameters affect the performance of resulting models, ranging from simple (surrogate-based) ablations (Fawcett & Hoos, 2016; Biedenkapp et al., 2017) to sensitivity analyses and eliciting interactions between hyperparameters based on the functional ANOVA framework (Hutter et al., 2014; van Rijn & Hutter, 2018; Bahmani et al., 2021; Watanabe et al., 2023). In this work, we propose a novel approach to quantifying HPI using Shapley values, with a particular focus on capturing interactions between hyperparameters through Shapley interaction indices. We focus on quantifying interactions since, in (Zimmer et al., 2021; Pushak & Hoos, 2022; Novello et al., 2023), it has been noticed that interaction is occasionally comparably low, which could serve as a foundation for a new generation of HPO methods that do not assume interactions to be omnipresent.

Beyond quantifying HPI, to better understand the impact of hyperparameters and the tuning behavior of hyperparameter optimizers, other approaches have been proposed, such as algorithm footprints (Smith-Miles & Tan, 2012), partial dependence plots for hyperparameter effects (Moosbauer et al., 2021) or deriving symbolic explanations (Segel et al., 2023), providing an interpretable model for estimating the performance of a learner from its hyperparameters. In this work, we focus on quantifying the impact of tuning a hyperparameter on the performance.

2. Hyperparameter Optimization

Hyperparameter optimization (HPO) is concerned with the problem of finding the most suitable hyperparameter configuration (HPC) of a learner for a given task, typically consisting of some labeled dataset D and some performance measure u quantifying the usefulness (Bischl et al., 2023). To put it more formally, let \mathcal{X} be an instance space and \mathcal{Y} a label space and suppose $x \in \mathcal{X}$ are (non-deterministically) associated with labels $y \in \mathcal{Y}$ via a joint probability distribution $P(\cdot, \cdot)$. Then, a dataset $D = \{(x^{(k)}, y^{(k)})\}_{k=1}^N \subset \mathcal{X} \times \mathcal{Y}$ is a sample from that probability distribution. Furthermore, a predictive performance measure $u : \mathcal{Y} \times P(\mathcal{Y}) \rightarrow \mathbb{R}$ is a function mapping tuples consisting of a label and a probability distribution over the label space to the reals. Given an HPC $\lambda \in \Lambda$, a learner parameterized with λ maps datasets D from the dataset space \mathbb{D} to a corresponding hypothesis $h_{\lambda, D} \in \mathcal{H} := \{h \mid h : \mathcal{X} \rightarrow P(\mathcal{Y})\}$.

As an HPC $\lambda \in \Lambda$ typically affects the hypothesis space \mathcal{H} and the learning behavior, it needs to be tuned to the given dataset and performance measure. The task of HPO is then to find an HPC yielding a hypothesis that generalizes well beyond the data used for training. For a dataset $D \in \mathbb{D}$, the following optimization problem needs to be solved:

$$\lambda^* \in \arg \max_{\lambda \in \Lambda} \int_{(x, y) \sim P(\cdot, \cdot)} u(y, h_{\lambda, D}(x)) .$$

As the true generalization performance is intractable, it is estimated by splitting the given dataset D into training D_T and validation data D_V . Accordingly, we obtain

$$\lambda^* \in \arg \max_{\lambda \in \Lambda} \text{VAL}_u(\lambda, D), \text{ with } \text{VAL}_u(\lambda, D) :=$$

$$\mathbb{E}_{(D_T, D_V) \sim D} \left[\frac{1}{|D_V|} \sum_{(x, y) \in D_V} u(y, h_{\lambda, D_T}(x)) \right].$$

Naively, hyperparameter optimization can be approached by discretizing the domains of hyperparameters and conducting a grid search or by a random search (Bergstra & Bengio, 2012). State-of-the-art methods leverage Bayesian optimization and multi-fidelity optimization for higher efficiency and effectiveness (Bischl et al., 2023).

3. Explainable AI (XAI) and Game Theory

Within the field of eXplainable AI (XAI), cooperative game theory has been widely applied to assign contributions to entities, such as features or data points for a given task (Rozemberczki et al., 2022). Most prominently, to interpret predictions of black box models using feature attributions (Lundberg & Lee, 2017) and the Shapley Value (SV) (Shapley, 1953). Shapley Interactions (SIs) (Grabisch & Roubens, 1999) extend the SV by additionally assigning contributions to groups of entities, which reveal *synergies and redundancies*. Such feature interactions uncover additive structures in predictions, which are necessary to understand complex decisions (Sundararajan et al., 2020). Overall, explanations are summarized by two components (Fumagalli et al., 2024a): First, an *explanation game* $\nu : 2^{\mathcal{N}} \rightarrow \mathbb{R}$ is defined as a real-valued set function over the powerset $2^{\mathcal{N}}$ of the n features of interest indexed by $\mathcal{N} = \{1, \dots, n\}$. This explanation game restricts the model prediction to subsets of features and evaluates a property of interest, e.g. the prediction or performance. Second, given an explanation game, *interpretable* main and interaction effects are constructed using the SV and SIs. Analogously, in Section 4, we define explanation games based on ablations of hyperparameters in VAL_u and quantify importances with the SV and SIs.

Explanation Games via Feature Imputations. Given the prediction of a black box model $f : \mathbb{R}^n \rightarrow \mathbb{R}$ and an instance $\mathbf{x} \in \mathbb{R}^n$, *baseline imputation* with $\mathbf{b} \in \mathbb{R}^n$ for a coalition $S \subseteq \mathcal{N}$ is given by $\oplus_S : \mathbb{R}^n \times \mathbb{R}^n \rightarrow \mathbb{R}^n$ as

$$\nu_{\mathbf{x}}^{(b)}(S) := f(\mathbf{x} \oplus_S \mathbf{b}) \text{ with } \mathbf{x} \oplus_S \mathbf{b} := \begin{cases} x_i, & \text{if } i \in S, \\ b_i, & \text{if } i \notin S. \end{cases}$$

Baseline imputation heavily depends on the choice of baseline (Sturmfels et al., 2020), and *marginal* and *conditional*

imputation extends the approach to an average over randomized baselines (Sundararajan & Najmi, 2020) as

$$\nu_{\mathbf{x}}^{(p)}(S) := \mathbb{E}_{\mathbf{b} \sim p(\mathbf{b})} [f(\mathbf{x} \oplus_S \mathbf{b})],$$

where $p(\mathbf{b})$ is either the marginal feature distribution or conditioned on $\mathbf{b} = \mathbf{x} \oplus_S \mathbf{b}$, respectively. Imputed model predictions define *local* explanation games that are used to explain predictions of single instances \mathbf{x} . In contrast, *global* explanation games capture derived properties, such as the variance or performance of the imputed model prediction. It was shown that explanations derived from baseline, marginal and conditional imputation are increasingly influenced by the feature distribution p (Fumagalli et al., 2024a).

Shapley Value (SV) and Shapley Interaction (SI). An explanation game is additively decomposed by the Möbius Interactions (MIs) $m : 2^{\mathcal{N}} \rightarrow \mathbb{R}$ (Muschalik et al., 2024a), i.e. the Möbius transform (Rota, 1964), for $T \subseteq \mathcal{N}$ as

$$\nu(T) = \sum_{S \subseteq T} m(S) \text{ with } m(S) := \sum_{L \subseteq S} (-1)^{|S|-|L|} \nu(L).$$

The MIs describe the *pure main and interaction effects*, but contain 2^n non-trivial components in ML applications (Muschalik et al., 2024a). As a remedy, the SV and SIs summarize the MIs into *interpretable* main and interaction effects of lower complexity. The SV assigns contributions to individuals and is uniquely characterized by four intuitive axioms: *linearity* (contributions are linear for linear combination of games), *symmetry* (players with equal contributions obtain equal payout), *dummy* (players that do not change the payout receive zero payout), and *efficiency* (the sum of all payouts equals the joint payout). The SV summarizes the MIs as $\phi^{\text{SV}}(i) = \sum_{S \subseteq \mathcal{N}: i \in S} \frac{1}{|S|} m(S)$ for all $i \in \mathcal{N}$. In other words, each MI is equally distributed among the involved players. Yet, the SV does not yield any insights into interactions. Given an *explanation order* $k \in \{1, \dots, n\}$, the SIs Φ_k extend the SV to assign contributions to subsets of players up to size k . For $k = 1$ the SIs yield the SV, whereas for $k = n$ the MIs. While there exist multiple variants of SIs, a positive interaction indicates a synergistic effect, whereas a negative interaction indicates redundancies (on average) of the involved features. For instance, the Faithful Shapley Interaction Index (FSII) (Tsai et al., 2023) is defined as the best k -additive approximation $\hat{\nu}_k(S) := \sum_{L \subseteq S: |L| \leq k} \Phi_k(L)$ of $\nu(S)$ across all subsets S weighted by the Shapley kernel, cf. Appendix D.2, which is useful to analyze the degree of interaction. The SIs adjust explanation expressivity and complexity based on practitioner needs, a framework we now parallel in HPO.

4. HYPERSHAP: Attributing Importance to Hyperparameters

In hyperparameter optimization (HPO), explanations are needed on different levels of the HPO process, ranging from returned configurations to a qualitative comparison of entire HPO tools. Here, we limit ourselves to four areas, dubbed Ablation, Sensitivity, Tunability, and Optimizer Bias. First, we introduce Ablation (Section 4.1), which we use as the fundamental backbone of HYPERSHAP. Based on Ablation, we discuss Sensitivity as an extension of the functional ANOVA framework by Hutter et al. (2014), and compare it theoretically to our novel approach for Tunability (Section 4.2). Tunability is then used to discover Optimizer Bias (Section 4.3), and we conclude with practical aspects of HYPERSHAP (Section 4.4). In the following, we let \mathcal{N} be the set of hyperparameters and quantify main and interaction effects based on the SV and SIs of the HPI games. All proofs are deferred to Appendix A.

4.1. Ablation of Hyperparameter Configurations

One common scenario for quantifying the HPI is to compare a hyperparameter configuration (HPC) λ^* of interest to some reference HPC λ^0 , e.g., the default parameterization of a learner as provided by its implementing library or a tuned default HPC that has proven effective for past tasks. In turn, λ^* can be any HPC obtained through HPO or a manual configuration. Given λ^* and λ^0 , the question now is how values of λ^* affect the performance of the learner relative to the reference HPC λ^0 . To this end, we can transition from the reference HPC to the HPC of interest by switching the values of hyperparameters one by one from its value in λ^0 to the value in λ^* , which is also done in empirical ML studies and referred to as ablations.

Ablation analysis has already been followed by Fawcett & Hoos (2016) and Biedenkapp et al. (2017) but restricted to single hyperparameter ablations that are executed sequentially. Instead, we consider the HPI game of Ablation using *all possible subsets*, which allows us to capture interactions.

Definition 4.1 (HPI Game - Ablation). The Ablation HPI game $\nu_{G_A} : 2^{\mathcal{N}} \rightarrow \mathbb{R}$ is defined based on a tuple

$$G_A := (\lambda^0, \lambda^*, D, u),$$

consisting of a *baseline (default)* HPC λ^0 , an HPC of interest λ^* , a dataset D , and a measure u . Given a coalition $S \subseteq \mathcal{N}$, we construct an intermediate HPC with $\oplus_S : \Lambda \times \Lambda \rightarrow \Lambda$ as

$$\lambda^* \oplus_S \lambda^0 := \begin{cases} \lambda_i^*, & \text{if } i \in S, \\ \lambda_i^0, & \text{else,} \end{cases}$$

and evaluate its worth with

$$\nu_{G_A}(S) := \text{VAL}_u(\lambda^* \oplus_S \lambda^0, D).$$

The Ablation game quantifies the worth of a coalition based on the comparison with a default HPC λ^0 . In XAI terminology, this approach is known as *baseline imputation*, cf. Section 3. Natural extensions of the Ablation game capture these ablations with respect to a distribution $\lambda^0 \sim p^0(\lambda^0)$ over the baseline HPC space Λ as

$$\mathbb{E}_{\lambda^0 \sim p^0(\lambda^0)}[\text{VAL}_u(\lambda^* \oplus_S \lambda^0, D)],$$

which relates to the *marginal performance* introduced by Hutter et al. (2014). In XAI terminology, it is further distinguished between distributions $p(\lambda^0)$ that either depend (conditional) or do not depend (marginal) on the HPC of interest λ^* . While baseline imputation is mostly chosen for computational efficiency, it was argued that it also satisfies beneficial properties (Sundararajan & Najmi, 2020). Nevertheless, the choice of a baseline has a strong impact on the explanation (Sturmfels et al., 2020). In HPO, we are typically given a *default* HPC λ^0 , which we use for the Ablation game, but our methodology can be directly extended to the probabilistic setting.

4.2. Tunability of Learners

Zooming out from a specific configuration, we can ask to what extent it is worthwhile to tune hyperparameters. In the literature, this question has been connected to the term of *tunability* (Probst et al., 2019). Tunability aims to quantify how much performance improvements can be obtained by tuning a learner comparing against a baseline HPC, e.g., an HPC that is known to work well across various datasets (Pushak & Hoos, 2020). In this context, we are interested in the importance of tuning specific hyperparameters. A classical tool to quantify variable importance is *sensitivity analysis* (Owen, 2013), which measures the variance induced by the variables of interest and decomposes their contributions into main and interaction effects.

Definition 4.2 (HPI Game - Sensitivity). The Sensitivity game $\nu_{G_V} : 2^{\mathcal{N}} \rightarrow \mathbb{R}$ is defined based on a tuple

$$G_V := (\lambda^0, \Lambda, p^*, D, u),$$

consisting of a *baseline* HPC λ^0 , an HPC space of interest Λ equipped with a probability distribution p^* , a dataset D , and a measure u . The value function is given by

$$\nu_{G_V}(S) := \mathbb{V}_{\lambda \sim p^*(\lambda)}[\text{VAL}_u(\lambda \oplus_S \lambda^0, D)].$$

A large value of a coalition $S \subseteq \mathcal{N}$ in the Sensitivity game indicates that these hyperparameters are important to be set to the right value. Hutter et al. (2014) implicitly rely on the Sensitivity game and compute the functional ANOVA decomposition, quantifying *pure* main and interaction effects. In game theory, this corresponds to the MIs of the Sensitivity game, which can be summarized into interpretable representations using the SV and SIs (Fumagalli et al., 2024a).

While sensitivity analysis is a suitable tool in XAI, it has some drawbacks for Tunability. First, as illustrated below, the total variance being decomposed $\nu_{G_V}(\mathcal{N})$ strongly depends on the chosen probability distribution p^* and the HPC space Λ . Moreover, it does not reflect the performance increase expected when tuning all hyperparameters. Second, for a coalition of hyperparameters $S \subseteq \mathcal{N}$, we expect that the coalition’s worth (performance) increases when tuning additional hyperparameters, i.e., $\nu(S) \leq \nu(T)$, if $S \subseteq T$. This property is known as *monotonicity* (Fujimoto et al., 2006), but *does not* hold in general for the Sensitivity game ν_{G_V} . For a simple example, we refer to Appendix A.3. Instead, we now propose the monotone Tunability HPI game.

Definition 4.3 (HPI Game - Tunability). The Tunability HPI game is defined by a tuple

$$G_T = (\lambda^0, \Lambda, D, u),$$

consisting of a baseline HPC $\lambda^0 \in \Lambda$, an HPC space Λ , a dataset D , and a measure u . The value function is given by

$$\nu_{G_T}(S) := \max_{\lambda \in \Lambda} \text{VAL}_u(\lambda \oplus_S \lambda^0, D).$$

The Tunability game directly measures the performance obtained from tuning the hyperparameters of a coalition S while leaving the remaining hyperparameters at the default value λ^0 . The Tunability game is monotone, which yields the following theorem.

Theorem 4.4. *The Tunability game yields non-negative SVs and non-negative pure individual (main) effects obtained from functional ANOVA via the MIs.*

While the main effects obtained from the Tunability game are non-negative, interactions clearly can be negative, indicating redundancies of the involved hyperparameters.

Benefits of Tunability over Sensitivity. We now showcase the benefits of the Tunability game over the Sensitivity game using a synthetic example. We consider a two-dimensional HPC space $\Lambda := \Lambda_1 \times \Lambda_2$ with discrete HPCs $\Lambda_1 := \{0, 1\}$ and $\Lambda_2 := \{0, \dots, m\}$ for $m > 1$. The optimal configuration is defined as $\lambda^* := (1, m)$, and the performance is quantified by $\text{VAL}_u(\lambda, D) := \mathbf{1}_{\lambda_1=\lambda_1^*} + \mathbf{1}_{\lambda_2=\lambda_2^*}$, where $\mathbf{1}$ is the indicator function. That is, we observe an increase of performance of 1 for each of the hyperparameters set to the optimal HPC λ^* . Lastly, we set the HPC baseline to $\lambda^0 := (0, 0)$ or $\lambda^0 := \lambda^*$. Intuitively, we expect that both hyperparameters obtain similar HPI scores, since they both contribute equally to the optimal performance $\text{VAL}_u(\lambda^*, D) = 2$. Moreover, if the baseline is set to the optimal HPC λ^* , we expect the HPI to reflect that there is no benefit of tuning. Since the hyperparameters independently affect the performance, we do not expect any interactions.

Table 1. HPI main and interaction effects of a two-dimensional synthetic HPO problem for the Sensitivity and Tunability game with baseline HPC set to $(0, 0)$ and the optimal HPC λ^* . The Sensitivity game assigns smaller contributions to hyperparameters with a larger domain (λ_2). Setting $\lambda^0 = \lambda^*$ reduces the Tunability HPI scores to zero, whereas Sensitivity is unaffected.

HPI Game		Sensitivity		Tunability	
λ^0		$(0, 0)$	λ^*	$(0, 0)$	λ^*
HPI	λ_1	1/4	1/4	1	0
	λ_2	$\frac{m}{(m+1)^2}$	$\frac{m}{(m+1)^2}$	1	0
	$\lambda_1 \times \lambda_2$	0	0	0	0

Theorem 4.5. *The HPI scores of the Sensitivity and Tunability game for the synthetic example are given by Table 1.*

Both HPI scores correctly quantify the absence of interaction $\lambda_1 \times \lambda_2$. In contrast to the Tunability game, the Sensitivity game assigns smaller HPI scores to the hyperparameter λ_2 due to the larger domain Λ_2 . In fact, the Sensitivity HPI score of λ_2 roughly decreases with order m^{-1} . Moreover, the Tunability HPI scores reflect the performance increase and decompose the difference between the optimal and the default performance. In contrast, the Sensitivity HPI scores decompose the overall variance, which depends on Λ and p^* . Lastly, setting the default HPC λ^0 to λ^* decreases the Tunability HPI scores to zero, whereas the Sensitivity HPI scores remain unaffected. In summary, Sensitivity reflects the variability in performance when changing the hyperparameters, whereas Tunability reflects the benefit of tuning.

4.3. Optimizer Bias

The Tunability game aims to explain the importance of hyperparameters being tuned, which can also be used to gain insights into the capabilities of a hyperparameter optimizer. In particular, by comparing the optimal performance with the empirical performance of a single optimizer, we uncover biases and point to specific hyperparameters that the optimizer fails to exploit. We define a hyperparameter optimizer as a function $\mathcal{O} : \mathbb{D} \times 2^\Lambda \rightarrow \Lambda$, mapping from the space of datasets and an HPC space to an HPC.

Definition 4.6 (HPI Game - Optimizer Bias). The Optimizer Bias HPI game is defined as a tuple

$$G_O = (\Lambda, \lambda^0, \mathcal{O}, D, u),$$

consisting of a HPC space Λ , a baseline λ^0 , the hyperparameter optimizer of interest \mathcal{O} , a dataset D and a measure u . For $S \subseteq \mathcal{N}$, we construct $\Lambda^S := \{\lambda \oplus_S \lambda^0 : \lambda \in \Lambda\}$ and define

$$\nu_{G_O}(S) := \text{VAL}_u(\mathcal{O}(D, \Lambda^S), D) - \nu_{G_T}(S).$$

Intuitively speaking, the value function measures any deviation from the performance of the actual best-performing HPC. In other words, with the help of Definition 4.6, we can identify deficiencies of the hyperparameter optimizer \mathcal{O} over the best-performing solution and, thereby for example, identify whether an optimizer struggles to optimize certain (types of) hyperparameters.

4.4. Practical Aspects of HYPERSHAP

This section addresses practical aspects of HYPERSHAP to efficiently approximate the proposed games and generalize them to multiple datasets.

Efficient Approximation. Naively, to evaluate a single coalition in Definition 4.3, we need to conduct one HPO run. While this can be costly, we argue that using surrogate models that are, e.g., obtained through Bayesian optimization, can be used to simulate HPO, rendering HYPERSHAP more tractable. This is similar to other surrogate-based explainability methods for HPO (Hutter et al., 2014; Biedenkapp et al., 2017; Moosbauer et al., 2021; Segel et al., 2023). In contrast, to analyze Optimizer Bias, we propose to approximate ν_{G_T} using a diverse ensemble of optimizers $\mathbb{O} := \{\mathcal{O}_i\}$, and choose the best result for Λ^S obtained through any optimizer from \mathbb{O} , forming a virtual optimizer that always yields the best-known value. This virtual best hyperparameter optimizer (VBO) approximates

$$\nu_{G_T}(S) \approx \max_{\lambda^i \in \mathcal{O}_i(D, \Lambda^S)} \text{VAL}_u(\lambda^i, D).$$

HPI Game Extensions across Multiple Datasets. In a more general setting, we are also interested in the different aspects of HYPERSHAP across multiple datasets, where we present direct extensions of the previous games.

Definition 4.7 (HPI Game- Multi-Dataset Variants). Given a collection of datasets $\mathcal{D} := \{D_1, \dots, D_M\}$ and the corresponding HPI games $\nu_G^{D_i}$ for $i \in \{1, \dots, M\}$ with $G \in \{G_A, G_V, G_T, G_O\}$, we define its multi-dataset variant with the value function

$$\nu_G^{\mathcal{D}}(S) := \bigoplus_{i=1}^M \nu_G^{D_i}(S),$$

where \bigoplus denotes an aggregation operator, e.g. the mean, of the game values obtained from the individual datasets D_i .

Considering HPI across datasets allows for a broader and more comprehensive assessment of the impact of individual hyperparameters and how they interact with each other. By aggregating the value of a coalition over datasets, we can evaluate the generalizability of HPI in contrast to identifying which hyperparameter is important for which dataset. For instance, this can justify recommendations with respect to

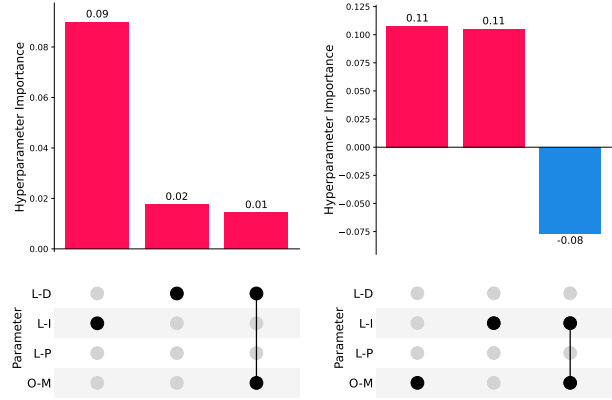


Figure 2. Upset plots (Lex et al., 2014) showing the hyperparameter importances for Ablation (left) and Tunability (right) wrt. lmlb_transformer from PD1 (Wang et al., 2024).

Multi-Data Tunability, which hyperparameters should be tuned in general. Alternatively, we can assure a systematic optimizer bias with respect to certain hyperparameters instead of observing data-specific effects only.

5. Experiments

In this section, we evaluate the effectiveness and applicability of HYPERSHAP across various scenarios. The experiments demonstrate how our games help explain HPIs, interactions, and biases in HPO. In all experiments we rely on four HPO benchmarks; lcbench (Zimmer et al., 2021), rbv2_ranger (Pfisterer et al., 2022), PD1 (Wang et al., 2024), and JAHS-Bench-201 (Bansal et al., 2022). The implementation is based around shapiq (Muschalik et al., 2024a). For more details regarding the experimental setup, we refer to Appendix B. Additional results are contained in Appendix E and a guide for interpreting interaction-based visualizations is presented in Appendix C. Generally, positive interactions are colored in red and negative in blue.

5.1. Insights from Ablation and Tunability

First, we compare the results of the Ablation and the Tunability game in terms of hyperparameter importance and interactions (cf. Figure 2). We retrieve an optimized configuration of PD1’s lmlb_transformer scenario and explain it with the Ablation game. HYPERSHAP’s explanation shows that the majority of the performance increase is attributed to the hyperparameter L-I, which is not surprising since the initial learning rate is also intuitively the most important one. However, using HYPERSHAP to create Tunability explanations reveals that both hyperparameters, L-I and O-M (optimizer momentum), are of equal importance with a negative interaction. This means that the optimizer chose to tune L-I over O-M for the configuration in question, even

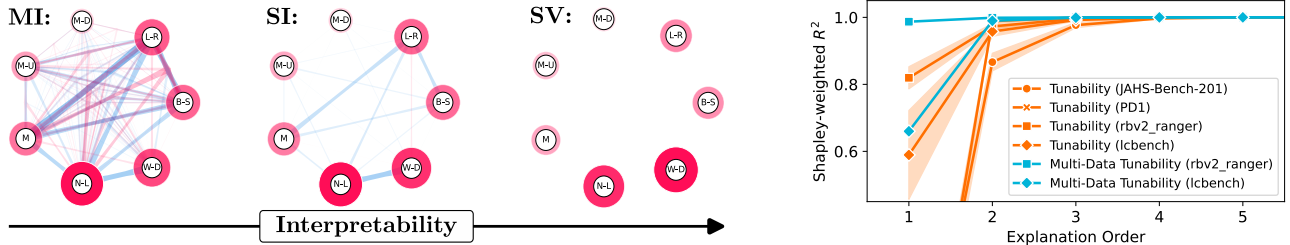


Figure 3. **Left:** Interaction graphs showing Möbius interactions (MI), Shapley interactions (SI), and Shapley values (SV) where pure MIs are summarized for improved interpretability via SIs and SVs. **Right:** Faithfulness of the lower-order explanations approximating higher-order effects (Muschalik et al., 2024a). An explanation order of 3 already closely approximates the full game ($R^2 \approx 1$).

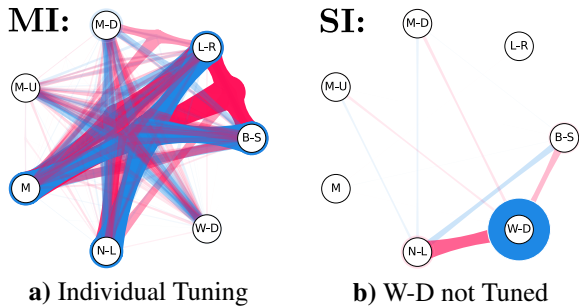


Figure 4. Interaction graphs showing results for the Optimizer Bias game via Moebius interactions (MI) and Shapley interactions (SI) on dataset ID 3945 of `lcbench`.

though a similar performance improvement could have been achieved by tuning O-M instead. Hence, HYPERSHAP is able to reveal which hyperparameters were subject to optimization via the Ablation game, while the Tunability game emphasizes the potential contributions of hyperparameters together with the interactions between them.

5.2. Higher-Order Interactions in HPO

Second, we investigate the interaction structure of the HPO problem. In Figure 3, left (MI), and further in Appendix E, we observe the presence of many higher-order interactions, which are difficult to interpret. The SIs (order 2) and SV in HYPERSHAP summarize the MI into *interpretable* explanations. Yet, Figure 3, right, shows that SIs still *faithfully* capture the overall game behavior, which we measure with a Shapley-weighted loss (Muschalik et al., 2024a) and varying explanation order (cf. Appendix D). We find that most of the explanatory power is captured by interactions up to the third order, confirming prior research that suggests hyperparameter interactions are typically of lower order (Pushak & Hoos, 2020). Interactions beyond the third order contribute little to the overall understanding of the game. Thanks to the convenient properties of the SV and SIs, HYPERSHAP provides a reliable way to capture and fairly summarize higher-order interactions into more interpretable explanations.

5.3. Detecting Optimizer Bias

The third experiment uses the Optimizer Bias game to uncover issues in black-box hyperparameter optimizers. To this end, we create two biased hyperparameter optimizers. The first optimizer tunes each hyperparameter separately, ignoring interactions between them, while the second is not allowed to tune the most important hyperparameter. Ideally, a perfect optimizer would show no interactions and no main effects in HYPERSHAP’s Optimizer Bias explanations.

Figure 4 shows the Optimizer Bias explanations, i.e., the difference between two Tunability games, using the optimizer’s returned value and the maximum, respectively. Since the main effects are always positive, the differences highlight the optimizer’s inability to properly tune certain hyperparameters. In Figure 4a, small main effects suggest that the optimizer can effectively tune hyperparameters individually, but the presence of both negative and positive interactions shows that it fails to capture these dependencies. This confirms the expectation that this optimizer, which tunes hyperparameters separately, fails to exploit synergies in tuning hyperparameters jointly. On the other hand, the second optimizer, ignoring the weight decay (W-D) hyperparameter for this particular dataset, clearly demonstrates bias in the interaction graph in Figure 4b. The blue main effect for W-D and interactions involving W-D reveal this bias, showing how HYPERSHAP can help identify such flaws and contribute to the development of more effective HPO methods.

5.4. Explaining the Surrogate During Optimization

Inspired by Rodemann et al. (2024), we explain SMAC (Lindauer et al., 2022), a state-of-the-art hyperparameter optimizer based on Bayesian optimization, using HYPERSHAP to analyze its surrogate model during the optimization procedure. We run SMAC (as pure black-box optimizer) with a budget of around 6 000 evaluations and investigate the surrogate model at 1%, 5%, 25%, and 100% of the budget. In Figure 5, we show how the model’s belief about

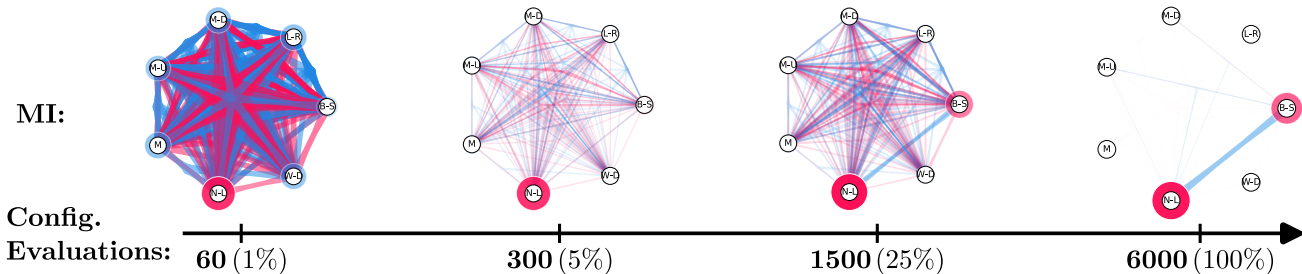


Figure 5. HYPERSHAP explains the surrogate model in SMAC’s Bayesian optimization at 1%, 5%, 25%, and 100% of the budget.

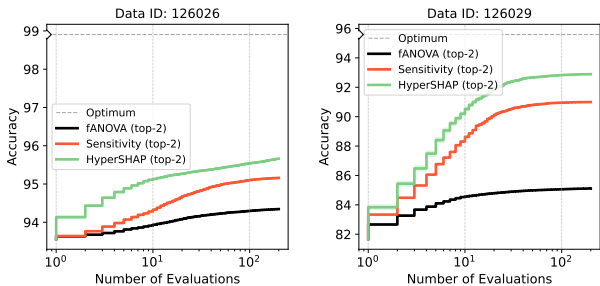


Figure 6. Anytime performance plots of hyperparameter optimization runs involving only the top-2 important hyperparameters for two datasets of `lcbench` (Zimmer et al., 2021).

HPI and interactions evolves. Initially uncertain, indicated by large interactions between hyperparameters, SMAC’s surrogate model successfully identifies the most important hyperparameters early on but requires a lot more evaluations to eventually learn the interaction effects correctly. This demonstrates the potential of HYPERSHAP to better understand what actually happens in HPO.

5.5. Comparison with Functional ANOVA (fANOVA)

Lastly, we design a validation task for hyperparameters deemed important by HYPERSHAP, and compare it to the well-known fANOVA framework (Hutter et al., 2014). To this end, for a given HPO task, we run fANOVA and HYPERSHAP using the SV with the Tunability and Sensitivity game to calculate the HPI of order 1. We then select the two most important hyperparameters and conduct an HPO run on a reduced HPC space containing only these two hyperparameters. We expect that HYPERSHAP achieves better performance for both the Tunability and Sensitivity game since the SV additionally reflects higher-order interactions. Moreover, the hyperparameters chosen based on the Tunability game are expected to outperform the selection based on the Sensitivity game. The results shown in Figure 6 (and further in Appendix E.2) confirm that the anytime performance of the runs informed by HYPERSHAP are clearly superior to those informed by fANOVA, and that

Tunability outperforms Sensitivity. This demonstrates that the HPI scores provided by HYPERSHAP are effectively contributing to maximizing the accuracy and thus guiding the optimization process. Furthermore, the optimization runs informed by fANOVA converge earlier than those of HYPERSHAP, supporting its capability to provide more actionable insights for HPO.

6. Conclusion

In this paper, we proposed HYPERSHAP, a post-hoc explanation framework for consistently and uniformly quantifying HPI using the SV and SIs across three levels: hyperparameter values, tunability of learners, optimizer capabilities. Unlike previous methods that quantify variance (Hutter et al., 2014; Watanabe et al., 2023), HYPERSHAP attributes performance contributions. We demonstrated that HYPERSHAP not only enhances understanding of the impact of hyperparameter values or tunability of learners but also provides actionable insights for subsequent HPO runs.

Limitations and Future Work. While HYPERSHAP reveals interesting insights into HPO, it is not directly clear how to utilize its explanations for the HPO process itself. This offers room for interesting future work as explanations can be computed in parallel and potentially guide the HPO tuner’s or AutoML framework’s search. Further, the computational bottleneck is the approximation of the $\arg \max$, requiring research on more efficient yet unbiased methods. In future work, we aim to extend the framework to combined algorithm selection and HPO, as well as the design of complete ML pipelines (Olson & Moore, 2016; Wever et al., 2018; Heffetz et al., 2020; Feurer et al., 2022). While these more complex AutoML scenarios are less explored, HYPERSHAP provides a versatile and theory-grounded approach for in-depth study. Additionally, we plan to develop HPO methods that utilize HPI, with the goal of learning across datasets to improve optimizer efficiency. This may allow warm-starting HPO in an interpretable way, complementing recent work on prior-guided HPO (Hvarfner et al., 2024) and human-centered AutoML (Lindauer et al., 2024).

Impact Statement

In conducting this research on HyperSHAP, we have carefully considered the ethical implications of our work. This paper presents work with the goal to advance the field of machine learning (ML) and specifically the field of explainable artificial intelligence (XAI) and hyperparameter optimization (HPO). There are many potential societal consequences of our work. The aim of our study is to improve the transparency and interpretability of hyperparameter optimization, which is crucial for building trust and accountability into hyperparameter optimization methods. Thus, our research impacts a wide variety of ML application domains and therein can positively impact ML adoption and potentially reveal biases or unwanted behavior in HPO systems.

However, we recognize that the increased explainability provided by XAI also carries ethical risks. There is the potential for “explainability-based white-washing”, where organizations, firms, or institutions might misuse XAI to justify questionable actions or outcomes. With responsible use, XAI can amplify the positive impacts of ML, ensuring its benefits are realized while minimizing harm.

References

- Bahmani, M., Shawi, R. E., Potikyan, N., and Sakr, S. To tune or not to tune? an approach for recommending important hyperparameters. *arXiv:2108.13066*, 2021.
- Bansal, A., Stoll, D., Janowski, M., Zela, A., and Hutter, F. JAHS-bench-201: A foundation for research on joint architecture and hyperparameter search. In Koyejo, S., Mohamed, S., Agarwal, A., Belgrave, D., Cho, K., and Oh, A. (eds.), *Proceedings of the 36th International Conference on Advances in Neural Information Processing Systems (NeurIPS’22)*, 2022.
- Bergstra, J. and Bengio, Y. Random search for hyperparameter optimization. *J. Mach. Learn. Res.*, 13:281–305, 2012.
- Biedenkapp, A., Lindauer, M., Eggensperger, K., Hutter, F., Fawcett, C., and Hoos, H. Efficient parameter importance analysis via ablation with surrogates. In Singh, S. and Markovitch, S. (eds.), *Proceedings of the Thirty-First AAAI Conference on Artificial Intelligence, February 4-9, 2017, San Francisco, California, USA*, pp. 773–779, 2017.
- Bischi, B., Binder, M., Lang, M., Pielok, T., Richter, J., Coors, S., Thomas, J., Ullmann, T., Becker, M., Boulesteix, A., Deng, D., and Lindauer, M. Hyperparameter optimization: Foundations, algorithms, best practices, and open challenges. *WIREs Data. Mining. Knowl. Discov.*, 13(2), 2023.
- Bordt, S. and von Luxburg, U. From Shapley Values to Generalized Additive Models and back. In *Proceedings of the International Conference on Artificial Intelligence and Statistics (AISTATS)*, pp. 709–745, 2023.
- Bouthillier, X. and Varoquaux, G. *Survey of Machine-learning Experimental Methods at NeurIPS2019 and ICLR2020*. PhD thesis, 2020.
- Charnes, A., Golany, B., Keane, M., and Rousseau, J. *Extremal Principle Solutions of Games in Characteristic Function Form: Core, Chebychev and Shapley Value Generalizations*, volume 11, pp. 123–133. 1988.
- Drozdal, J., Weisz, J., Wang, D., Dass, G., Yao, B., Zhao, C., Muller, M., Ju, L., and Su, H. Trust in AutoML: Exploring information needs for establishing trust in automated machine learning systems. In Paternò, F., Oliver, N., Conati, C., Spano, L. D., and Tintarev, N. (eds.), *IUI ’20: 25th International Conference on Intelligent User Interfaces, Cagliari, Italy, March 17-20, 2020*, pp. 297–307, 2020.
- Fawcett, C. and Hoos, H. Analysing differences between algorithm configurations through ablation. *J. Heuristics*, 22(4):431–458, 2016.
- Feurer, M., Klein, A., Eggensperger, K., Springenberg, J. T., Blum, M., and Hutter, F. Efficient and robust automated machine learning. In Cortes, C., Lawrence, N., Lee, D., Sugiyama, M., and Garnett, R. (eds.), *Advances in Neural Information Processing Systems 28: Annual Conference on Neural Information Processing Systems 2015, December 7-12, 2015, Montreal, Quebec, Canada*, pp. 2962–2970, 2015.
- Feurer, M., Eggensperger, K., Falkner, S., Lindauer, M., and Hutter, F. Auto-sklearn 2.0: Hands-free AutoML via meta-learning. *J. Mach. Learn. Res.*, 23:261:1–261:61, 2022.
- Fujimoto, K., Kojadinovic, I., and Marichal, J. Axiomatic Characterizations of Probabilistic and Cardinal-probabilistic Interaction indices. *Games and Economic Behavior*, 55(1):72–99, 2006.
- Fumagalli, F., Muschalik, M., Hüllermeier, E., Hammer, B., and Herbinger, J. Unifying Feature-based Explanations With Functional ANOVA and Cooperative Game Theory, 2024a.
- Fumagalli, F., Muschalik, M., Kolpaczki, P., Hüllermeier, E., and Hammer, B. Kernelshap-iq: Weighted least square optimization for shapley interactions. In *Forty-first International Conference on Machine Learning, ICML 2024, Vienna, Austria, July 21-27, 2024*, 2024b.

- Grabisch, M. *Set Functions, Games and Capacities in Decision Making*, volume 46. 2016.
- Grabisch, M. and Roubens, M. An Axiomatic Approach to the Concept of Interaction Among Players in Cooperative games. *International Journal of Game Theory*, 28(4): 547–565, 1999.
- Hasebrook, N., Morsbach, F., Kannengießer, N., Zöller, M., Franke, J., Lindauer, M., Hutter, F., and Sunyaev, A. Practitioner motives to select hyperparameter optimization methods. *arXiv:2203.01717*, 2023.
- Heffetz, Y., Vainshtein, R., Katz, G., and Rokach, L. DeepLine: AutoML tool for pipelines generation using deep reinforcement learning and hierarchical actions filtering. In Gupta, R., Liu, Y., Tang, J., and Prakash, B. A. (eds.), *KDD '20: The 26th ACM SIGKDD Conference on Knowledge Discovery and Data Mining*, pp. 2103–2113, 2020.
- Hutter, F., Hoos, H., and Leyton-Brown, K. An efficient approach for assessing hyperparameter importance. In *Proceedings of the 31th International Conference on Machine Learning, ICML 2014, Beijing, China, 21-26 June 2014*, volume 32, pp. 754–762, 2014.
- Hvarfner, C., Hutter, F., and Nardi, L. A general framework for user-guided bayesian optimization. In *The Twelfth International Conference on Learning Representations, ICLR, 2024*.
- Lee, D. J. L., Macke, S., Xin, D., Lee, A., Huang, S., and Parameswaran, A. A human-in-the-loop perspective on AutoML: Milestones and the road ahead. *IEEE Data Eng. Bull.*, 42(2):59–70, 2019.
- Lex, A., Gehlenborg, N., Strobel, H., Vuillemot, R., and Pfister, H. UpSet: Visualization of intersecting sets. *IEEE Transactions on Visualization and Computer Graphics*, 20(12):1983–1992, 2014.
- Lindauer, M., Eggenberger, K., Feurer, M., Biedenkapp, A., Deng, D., Benjamins, C., Ruhkopf, T., Sass, R., and Hutter, F. SMAC3: A versatile bayesian optimization package for hyperparameter optimization. *Journal of Machine Learning Research*, 23(54):1–9, 2022.
- Lindauer, M., Karl, F., Klier, A., Moosbauer, J., Tornede, A., Müller, A., Hutter, F., Feurer, M., and Bischl, B. Position: A call to action for a human-centered AutoML paradigm. In *Forty-first International Conference on Machine Learning, ICML, 2024*.
- Lundberg, S. and Lee, S. A Unified Approach to Interpreting Model Predictions. In *Proceedings of Advances in Neural Information Processing Systems (NeurIPS)*, pp. 4765–4774, 2017.
- Moosbauer, J., Herbinger, J., Casalicchio, G., Lindauer, M., and Bischl, B. Explaining hyperparameter optimization via partial dependence plots. In Ranzato, M., Beygelzimer, A., Dauphin, Y., Liang, P., and Vaughan, J. W. (eds.), *Advances in Neural Information Processing Systems 34: Annual Conference on Neural Information Processing Systems 2021, NeurIPS 2021, December 6-14, 2021, virtual*, pp. 2280–2291, 2021.
- Muschalik, M., Baniecki, H., Fumagalli, F., Kolpaczki, P., Hammer, B., and Hüllermeier, E. Shapiq: Shapley interactions for machine learning. In *The Thirty-eight Conference on Neural Information Processing Systems Datasets and Benchmarks Track, 2024a*.
- Muschalik, M., Fumagalli, F., Hammer, B., and Hüllermeier, E. Beyond TreeSHAP: Efficient computation of any-order shapley interactions for tree ensembles. In *Thirty-Eighth AAAI Conference on Artificial Intelligence, (AAAI 2024)*, pp. 14388–14396, 2024b.
- Novello, P., Poëtte, G., Lugato, D., and Congedo, P. M. Goal-oriented sensitivity analysis of hyperparameters in deep learning. *J. Sci. Comput.*, 94(3):45, 2023.
- Olson, R. and Moore, J. TPOT: A tree-based pipeline optimization tool for automating machine learning. In Hutter, F., Kotthoff, L., and Vanschoren, J. (eds.), *Proceedings of the 2016 Workshop on Automatic Machine Learning*, volume 64, pp. 66–74, 2016.
- Owen, A. Variance Components and Generalized Sobol’ Indices. *SIAM/ASA Journal on Uncertainty Quantification*, 1(1):19–41, 2013.
- Pfisterer, F., Schneider, L., Moosbauer, J., Binder, M., and Bischl, B. YAHPO gym - an efficient multi-objective multi-fidelity benchmark for hyperparameter optimization. In Guyon, I., Lindauer, M., van der Schaar, M., Hutter, F., and Garnett, R. (eds.), *International Conference on Automated Machine Learning, AutoML 2022, 25-27 July 2022, Johns Hopkins University, Baltimore, MD, USA*, volume 188, pp. 3/1–39, 2022.
- Probst, P., Boulesteix, A., and Bischl, B. Tunability: Importance of hyperparameters of machine learning algorithms. *J. Mach. Learn. Res.*, 20:53:1–53:32, 2019.
- Pushak, Y. and Hoos, H. Golden parameter search: Exploiting structure to quickly configure parameters in parallel. In Coello, C. A. C. (ed.), *GECCO '20: Genetic and Evolutionary Computation Conference, Cancún Mexico, July 8-12, 2020*, pp. 245–253, 2020.
- Pushak, Y. and Hoos, H. AutoML loss landscapes. *ACM Trans. Evol. Learn. Optim.*, 2(3):10:1–10:30, 2022.

- Rodemann, J., Croppi, F., Arens, P., Sale, Y., Herbinger, J., Bischl, B., Hüllermeier, E., Augustin, T., Walsh, C. J., and Casalicchio, G. Explaining bayesian optimization by shapley values facilitates human-ai collaboration. *CoRR*, abs/2403.04629, 2024. doi: 10.48550/ARXIV.2403.04629. URL <https://doi.org/10.48550/arXiv.2403.04629>.
- Rota, G. On the foundations of combinatorial theory: I. theory of möbius functions. In *Classic Papers in Combinatorics*, pp. 332–360. 1964.
- Rozemberczki, B., Watson, L., Bayer, P., Yang, H., Kiss, O., Nilsson, S., and Sarkar, R. The shapley value in machine learning. In *Proceedings of International Joint Conference on Artificial Intelligence (IJCAI)*, pp. 5572–5579, 2022.
- Schneider, L., Schäpermeier, L., Prager, R. P., Bischl, B., Trautmann, H., and Kerschke, P. HPO \times ELA: investigating hyperparameter optimization landscapes by means of exploratory landscape analysis. In Rudolph, G., Kononova, A., Aguirre, H., Kerschke, P., Ochoa, G., and Tusar, T. (eds.), *Parallel Problem Solving from Nature - PPSN XVII - 17th International Conference, PPSN 2022, Dortmund, Germany, September 10-14, 2022, Proceedings, Part I*, volume 13398, pp. 575–589, 2022.
- Segel, S., Graf, H., Tornede, A., Bischl, B., and Lindauer, M. Symbolic explanations for hyperparameter optimization. In Faust, A., Garnett, R., White, C., Hutter, F., and Gardner, J. (eds.), *International Conference on Automated Machine Learning, 12-15 November 2023, Hasso Plattner Institute, Potsdam, Germany*, volume 224, pp. 2/1–22, 2023.
- Shapley, L. A Value for N-person Games. In *Contributions to the Theory of Games (AM-28), Volume II*, pp. 307–318. 1953.
- Simon, S., Kolyada, N., Akiki, C., Potthast, M., Stein, B., and Siegmund, N. Exploring hyperparameter usage and tuning in machine learning research. In *2nd IEEE/ACM International Conference on AI Engineering - Software Engineering for AI, CAIN 2023, Melbourne, Australia, May 15-16, 2023*, pp. 68–79, 2023.
- Smith-Miles, K. and Tan, T. Measuring algorithm footprints in instance space. In *Proceedings of the IEEE Congress on Evolutionary Computation, CEC 2012, Brisbane, Australia, June 10-15, 2012*, pp. 1–8, 2012.
- Snoek, J., Swersky, K., Zemel, R., and Adams, R. Input warping for bayesian optimization of non-stationary functions. In *Proceedings of the 31th International Conference on Machine Learning, ICML 2014, Beijing, China, 21-26 June 2014*, volume 32, pp. 1674–1682, 2014.
- Sturmfels, P., Lundberg, S., and Lee, S. Visualizing the Impact of Feature Attribution Baselines. *Distill*, 2020. <https://distill.pub/2020/attribution-baselines>.
- Sun, Y., Song, Q., Gui, X., Ma, F., and Wang, T. AutoML in the wild: Obstacles, workarounds, and expectations. In Schmidt, A., Väänänen, K., Goyal, T., Kristensson, P. O., Peters, A., Mueller, S., Williamson, J., and Wilson, M. (eds.), *Proceedings of the 2023 CHI Conference on Human Factors in Computing Systems, CHI 2023, Hamburg, Germany, April 23-28, 2023*, pp. 247:1–247:15, 2023.
- Sundararajan, M. and Najmi, A. The Many Shapley Values for Model Explanation. In *Proceedings of the International Conference on Machine Learning (ICML)*, pp. 9269–9278, 2020.
- Sundararajan, M., Dhamdhere, K., and Agarwal, A. The Shapley Taylor Interaction Index. In *Proceedings of the International Conference on Machine Learning (ICML)*, pp. 9259–9268, 2020.
- Theodorakopoulos, D., Stahl, F., and Lindauer, M. Hyperparameter importance analysis for multi-objective AutoML. *arXiv:2405.07640*, 2024.
- Tribes, C., Benarroch-Lelong, S., Lu, P., and Kobayev, I. Hyperparameter optimization for large language model instruction-tuning. *arXiv:2312.00949*, 2023.
- Tsai, C., Yeh, C., and Ravikumar, P. Faith-Shap: The Faithful Shapley Interaction Index. *Journal of Machine Learning Research*, 24(94):1–42, 2023.
- van Rijn, J. and Hutter, F. Hyperparameter importance across datasets. In Guo, Y. and Farooq, F. (eds.), *Proceedings of the 24th ACM SIGKDD International Conference on Knowledge Discovery & Data Mining, KDD 2018, London, UK, August 19-23, 2018*, pp. 2367–2376, 2018.
- Wang, C., Liu, X., and Awadallah, A. H. Cost-effective hyperparameter optimization for large language model generation inference. In Faust, A., Garnett, R., White, C., Hutter, F., and Gardner, J. (eds.), *International Conference on Automated Machine Learning, 12-15 November 2023, Hasso Plattner Institute, Potsdam, Germany*, volume 224, pp. 21/1–17, 2023.
- Wang, D., Weisz, J., Muller, M., Ram, P., Geyer, W., Dugan, C., Tausczik, Y., Samulowitz, H., and Gray, A. Human-ai collaboration in data science: Exploring data scientists’ perceptions of automated AI. *Proc. ACM Hum. Comput. Interact.*, 3(CSCW):211:1–211:24, 2019.
- Wang, Z., Dahl, G., Swersky, K., Lee, C., Mariet, Z., Nado, Z., Gilmer, J., Snoek, J., and Ghahramani, Z. Pre-trained Gaussian processes for Bayesian optimization. *J. Mach. Learn. Res.*, 2024.

- Watanabe, S., Bansal, A., and Hutter, F. PED-ANOVA: efficiently quantifying hyperparameter importance in arbitrary subspaces. In *Proceedings of the Thirty-Second International Joint Conference on Artificial Intelligence, IJCAI 2023, 19th-25th August 2023, Macao, SAR, China*, pp. 4389–4396, 2023.
- Wever, M., Mohr, F., and Hüllermeier, E. ML-Plan for unlimited-length machine learning pipelines. In *ICML 2018 AutoML Workshop*, 2018.
- Wever, M., Tornede, A., Mohr, F., and Hüllermeier, E. AutoML for multi-label classification: Overview and empirical evaluation. *IEEE Trans. Pattern Anal. Mach. Intell.*, 43(9):3037–3054, 2021.
- Xin, D., Wu, E. Y., Lee, D. J. L., Salehi, N., and Parameswaran, A. Whither AutoML? understanding the role of automation in machine learning workflows. In Kitamura, Y., Quigley, A., Isbister, K., Igarashi, T., Bjørn, P., and Drucker, S. M. (eds.), *CHI '21: CHI Conference on Human Factors in Computing Systems, Virtual Event / Yokohama, Japan, May 8-13, 2021*, pp. 83:1–83:16, 2021.
- Yin, Y., Chen, C., Shang, L., Jiang, X., Chen, X., and Liu, Q. AutoTinyBERT: Automatic hyper-parameter optimization for efficient pre-trained language models. In Zong, C., Xia, F., Li, W., and Navigli, R. (eds.), *Proceedings of the 59th Annual Meeting of the Association for Computational Linguistics and the 11th International Joint Conference on Natural Language Processing, ACL/IJCNLP 2021, (Volume 1: Long Papers), Virtual Event, August 1-6, 2021*, pp. 5146–5157, 2021.
- Zimmer, L., Lindauer, M., and Hutter, F. Auto-pytorch tabular: Multi-fidelity MetaLearning for efficient and robust AutoDL. *IEEE Transactions on Pattern Analysis and Machine Intelligence*, pp. 3079 – 3090, 2021. also available under <https://arxiv.org/abs/2006.13799>.

Organization of the Supplemental Material

The technical supplement is organized as follows.

A Proofs	14
A.1 Proof of Theorem 4.4	14
A.2 Proof of Theorem 4.5	14
A.3 Example: Non-Monotone Sensitivity Game	15
B Experimental Setup	16
B.1 Considered Benchmarks	16
B.2 Approximation of the argmax	17
B.3 Computing Optimizer Bias	17
B.4 Hardware Usage and Compute Resources	18
C Guidance on Interpreting Interaction Visualizations	19
D Interaction Quantification in Hyperparameter Optimization	20
D.1 Measuring the Magnitude of Interactions	20
D.2 Analyzing Lower-Order Representations of Games	20
D.3 Additional Experimental Details	21
E Additional Empirical Results	22
E.1 Additional Information for the Comparison of Ablation and Tunability	22
E.2 Additional Results for Comparison with fANOVA	22
E.3 Additional Results for Explaining the SMAC Surrogate During Optimization	23
E.4 Additional Interaction Visualizations	23

A. Proofs

A.1. Proof of Theorem 4.4

Proof. The Tunability game is given by the value function

$$\nu(S) := \nu_{G_T}(S) := \max_{\lambda \in \Lambda} \text{VAL}_u(\lambda \oplus_S \lambda^0, D).$$

We now want to show monotonicity of the value function, i.e., $S \subseteq T$ implies $\nu(S) \leq \nu(T)$. Given a coalition $T \subseteq \mathcal{N}$ with $S \subseteq T$, we immediately see that

$$A := \{\lambda \oplus_S \lambda^0 : \lambda \in \Lambda\} \subseteq \{\lambda \oplus_T \lambda^0 : \lambda \in \Lambda\} =: B,$$

since we can set the hyperparameters of $T \setminus S$ to $\lambda^0 \in \Lambda$ on the right-hand side. Since the Tunability game takes the max over these two sets, respectively, we obtain

$$\nu(S) = \max_{\lambda \in \Lambda} \text{VAL}_u(\lambda \oplus_S \lambda^0, D) = \max_{\lambda^* \in A} \text{VAL}_u(\lambda^*, D) \stackrel{A \subseteq B}{\leq} \max_{\lambda^* \in B} \text{VAL}_u(\lambda^*, D) = \max_{\lambda \in \Lambda} \text{VAL}_u(\lambda \oplus_T \lambda^0, D) = \nu(T).$$

This concludes that the Tunability game is monotone. As a consequence, we obtain non-negative SVs due to the *monotonicity* axiom (Fujimoto et al., 2006) of the SV. We can also give a direct proof of this via the well-known representation of the SV in terms of a weighted average over marginal contributions as

$$\phi^{\text{SV}}(i) := \sum_{T \subseteq \mathcal{N} \setminus \{i\}} \frac{1}{n \cdot \binom{n-1}{|T|}} (\nu(T \cup \{i\}) - \nu(T)).$$

Due to the monotonicity of ν_{G_T} , it follows that $\nu_{G_T}(T) \leq \nu_{G_T}(T \cup i)$, and thus all terms in the above sum are non-negative. Consequently, the SV is non-negative.

Moreover, the pure individual (main) effects obtained from the functional ANOVA framework are represented by the MI of the individuals (Fumagalli et al., 2024a). By the monotonicity of ν , we obtain again

$$m(i) := \nu(i) - \nu(\emptyset) \geq 0,$$

which concludes the proof. \square

A.2. Proof of Theorem 4.5

Proof. Given the synthetic Tunability and Sensitivity game with two dimensions $\mathcal{N} = \{1, 2\}$, our goal is to show that the main and interaction effects are given by Table 1.

Tunability Game. We first proceed to compute the game values of the Tunability game for $S \subseteq \mathcal{N}$ with the optimal HPC $\lambda^* = (1, m)$ as

$$\nu_{G_T}(S) = \max_{\lambda \in \Lambda} \text{VAL}_u(\lambda \oplus_S \lambda^0, D) = \text{VAL}_u(\lambda^* \oplus_S \lambda^0, D) = \sum_{i \in \{1, 2\}} \mathbf{1}_{(\lambda \oplus_S \lambda^0)_i = \lambda_i^*} = |S| + \sum_{i \in \mathcal{N} : i \notin S} \mathbf{1}_{\lambda_i^0 = \lambda_i^*}. \quad (1)$$

For the baseline set to $\lambda^0 := (0, 0)$, the second sum in Equation (1) vanishes and we thus obtain

$$\nu_{G_T}(S) = \begin{cases} 0, & \text{if } S = \emptyset, \\ 1, & \text{if } |S| = 1, \\ 2, & \text{if } S = \{1, 2\}. \end{cases}$$

Hence, the MIs are given by

$$m_{G_T}(S) = \sum_{L \subseteq S} (-1)^{|S|-|L|} \nu_{G_T}(L) = \begin{cases} 0, & \text{if } S = \emptyset, \\ 1, & \text{if } |S| = 1, \\ 0, & \text{if } S = \{1, 2\}. \end{cases}$$

Clearly, the interaction $\lambda_1 \times \lambda_2$, i.e., $m(\{1, 2\})$, vanishes, and thus the HPI scores of the individuals are given by their main effects in terms of the MIs. In summary, the HPI main effects using the SV and the MI are both equal to 1, whereas the interaction is zero, confirming the values shown in Table 1.

For the baseline set to $\lambda^0 := \lambda^*$, the second sum in Equation (1) equals $|\mathcal{N}| - |S|$ and thus we obtain a constant game

$$\nu_{G_T}(S) = |S| + |\mathcal{N}| - |S| = 2 \text{ for all } S \subseteq \mathcal{N}.$$

Consequently, all interactions and main effects are zero due to the dummy axiom (Fujimoto et al., 2006), confirming Table 1.

Sensitivity Game. We now proceed to compute the game values of the Sensitivity game for $S \subseteq \mathcal{N}$. First, for $S = \emptyset$, we obtain $\nu_{G_V}(\emptyset) = 0$, since $\lambda \oplus_{\emptyset} \lambda^0 = \lambda^0$, and thus there is no variance with respect to λ . Due to independence of the hyperparameter distribution, we can decompose the variance as

$$\nu_{G_V}(S) = \mathbb{V}_{\lambda^* \sim p(\lambda^*)}[\text{VAL}_u(\lambda^* \oplus_S \lambda^0, D)] = \mathbb{V}_{\lambda^* \sim p(\lambda^*)} \left[\sum_{i \in \{1, 2\}} \mathbf{1}_{(\lambda^* \oplus_S \lambda^0)_i = \lambda_i^0} \right] = \sum_{i \in S} \mathbb{V}_{\lambda_i^* \sim p(\lambda_i^*)} [\mathbf{1}_{(\lambda^* \oplus_S \lambda^0)_i = \lambda_i^0}] \quad (2)$$

To compute $\mathbb{V}_{\lambda_i^* \sim p(\lambda_i^*)} [\mathbf{1}_{(\lambda^* \oplus_S \lambda^0)_i = \lambda_i^0}]$, we note that $\mathbf{1}_{(\lambda^* \oplus_S \lambda^0)_i = \lambda_i^0}$ is described by a Bernoulli variable.

Given any baseline, we have $\mathbf{1}_{(\lambda^* \oplus_S \lambda^0)_i = \lambda_i^0} \sim \text{Ber}(q_i)$ with $q_1 = 1/2$ and $q_2 = 1/(m+1)$ due to the uniform distribution, which sets this value to 1, if the optimal HPC value is chosen. The variance of this Bernoulli variable is then given by $q(1-q)$, which yields

$$\mathbb{V}_{\lambda_i^* \sim p(\lambda_i^*)} [\mathbf{1}_{(\lambda^* \oplus_S \lambda^0)_i = \lambda_i^0}] = \begin{cases} \frac{1}{4}, & \text{if } i = 1, \\ \frac{1}{m+1} \left(1 - \frac{1}{m+1}\right) = \frac{m}{(m+1)^2}, & \text{if } i = 2, \end{cases}$$

which yields the game values

$$\nu_{G_V}(S) = \begin{cases} 0, & \text{if } S = \emptyset, \\ \frac{1}{4}, & \text{if } S = \{1\}, \\ \frac{m}{(m+1)^2}, & \text{if } S = \{2\}, \\ \frac{1}{4} + \frac{m}{(m+1)^2}, & \text{if } S = \{1, 2\}. \end{cases}$$

Hence, the MIs are given by

$$m_{G_V}(S) = \sum_{L \subseteq S} (-1)^{|S|-|L|} \nu_{G_V}(L) = \begin{cases} 0, & \text{if } S = \emptyset, \\ \frac{1}{4}, & \text{if } S = \{1\}, \\ \frac{m}{(m+1)^2}, & \text{if } S = \{2\}, \\ 0, & \text{if } S = \{1, 2\}, \end{cases}$$

which confirms the values given in Table 1 and concludes the proof. \square

A.3. Example: Non-Monotone Sensitivity Game

In this section, we give an example of a non-monotone Sensitivity game. To this end, we consider two hyperparameters $\mathcal{N} = \{1, 2\}$ equipped with independent Bernoulli distributions $\lambda_1, \lambda_2 \stackrel{\text{iid}}{\sim} \text{Ber}(1/2)$. We consider a performance measure as

$$\text{VAL}_u(\lambda) := \mathbf{1}_{\lambda_1=0} \mathbf{1}_{\lambda_2=0},$$

and set the baseline HPC to $\lambda^0 := (0, 0)$. The Sensitivity game values are then computed by observing that $\text{VAL}_u(\lambda^*)$ with $\lambda^* \sim p^*(\lambda^*)$ is described as a Bernoulli variable $\text{Ber}(q)$. For $S = \{1, 2\}$, the probability of VAL_u being 1 is $q = 1/4$, since both hyperparameters have to be set to zero. In contrast, for $|S| = 1$, we have $q = 1/2$, since the remaining variable is already set at zero due to the baseline HPC. We thus obtain again the variances with $q(1-q)$ as

$$\nu_{G_V}(S) = \mathbb{V}_{\lambda^* \sim p^*(\lambda^*)} [\mathbf{1}_{\lambda_1^*=0} \mathbf{1}_{\lambda_2^*=0}] = \begin{cases} 0, & \text{if } S = \emptyset, \\ \frac{1}{2} \frac{1}{2} = \frac{1}{4}, & \text{if } |S| = 1, \\ \frac{1}{4} \frac{3}{4} = \frac{3}{16}, & \text{if } S = \{1, 2\}. \end{cases}$$

Hence, we obtain that $\nu_{G_V}(\{1\}) = 1/4 \geq 3/16 = \nu_{G_V}(\{1, 2\})$, which shows that ν_{G_V} is not monotone.

B. Experimental Setup

Our implementation builds upon the `shapiq` package (Muschalik et al., 2024a), which is publicly available on GitHub¹, for computing Shapley values and interactions. Furthermore, for the experiments, we use YAHPO-Gym (Pfisterer et al., 2022), a surrogate-based benchmark for multi-fidelity hyperparameter optimization. YAHPO-Gym provides several benchmark suites, i.a., `lcbench` (Zimmer et al., 2021), which we focused on in the main paper. However, in the subsequent sections, we also present results from the `rbv2_ranger` benchmark set, a random forest benchmark, from YAHPO-Gym demonstrating the more general applicability of HYPERSHAP. Furthermore, we run evaluations on the benchmark `PD1` and `JAHS-Bench-201` to showcase HYPERSHAP’s wide applicability. In our repository, we provide pre-computed games to foster reproducibility of our results and allow for faster post-processing of the game values, e.g., for plotting different representations of the played games.

For better readability in terms of the font size, hyperparameter names are abbreviated in the interaction graphs.

B.1. Considered Benchmarks

lcbench (Pfisterer et al., 2022; Zimmer et al., 2021). `lcbench` is a benchmark considering joint optimization of the neural architecture and hyperparameters that has been proposed by (Zimmer et al., 2021) together with the automated deep learning system Auto-PyTorch. The benchmark consists of 35 datasets with 2000 configurations each for which the learning curves have been recorded, allowing for benchmarking multi-fidelity HPO. However, in YAHPO-Gym only 34 of the 35 original datasets are contained which is why our evaluation is also restricted to those 34 datasets.

Hyperparameter Name	Abbreviation	Type
<code>weight_decay</code>	W-D	float
<code>learning_rate</code>	L-R	float
<code>num_layers</code>	N-L	integer
<code>momentum</code>	M	float
<code>max_dropout</code>	M-D	float
<code>max_units</code>	M-U	integer
<code>batch_size</code>	B-S	float

rbv2_ranger (Pfisterer et al., 2022). As already mentioned above, `rbv2_ranger` is a benchmark faced with tuning the hyperparameters of a random forest. We consider the hyperparameters of `ranger` as listed below:

Hyperparameter Name	Abbreviation	Type
<code>min_node_size</code>	M-N	integer
<code>mtry_power</code>	M-P	float
<code>num_impute_selected_cpo</code>	N-I	categorical
<code>num_trees</code>	N-T	integer
<code>respect_unordered_factors</code>	R-U	categorical
<code>sample_fraction</code>	S-F	float
<code>splitrule</code>	S	categorical/Boolean
<code>num_random_splits</code>	N-R	integer

PD1 (Wang et al., 2024). The `PD1` benchmark is a testbed for evaluating hyperparameter optimization methods in the deep learning domain. It consists of tasks derived from realistic hyperparameter tuning problems, including transformer models and image classification networks. Across these different types of models, 4 hyperparameters are subject to tuning:

¹<https://github.com/mmschlk/shapiq>

Hyperparameter Name	Abbreviation	Type
lr_decay_factor	L-D	float
lr_initial	L-I	float
lr_power	L-P	float
opt_momentum	O-M	float

JAHS-Bench-201 (Bansal et al., 2022). To democratize research on neural architecture search, various table look-up and surrogate-based benchmarks have been proposed in the literature. Going even beyond plain neural architecture search, in JAHS-Bench-201, the combined task of searching for a suitable neural architecture and optimizing the hyperparameters of the learning algorithm is considered. We include it via the “mf-prior-bench” package that serves it with a surrogate model for predicting the validation error of a given architecture and hyperparameter configuration. The considered hyperparameters, including those for the neural architecture, are as follows:

Hyperparameter Name	Abbreviation	Type
Activation	A	categorical
LearningRate	L	float
Op1	Op1	categorical
Op2	Op2	categorical
Op3	Op3	categorical
Op4	Op4	categorical
Op5	Op5	categorical
Op6	Op6	categorical
TrivialAugment	T	Boolean
WeightDecay	W	float

B.2. Approximation of the argmax

As per Definition 4.3 to Definition 4.6, for every coalition S , we need to determine the arg max. However, the true arg max is difficult to determine, so we approximate it throughout our experiments. For the sake of implementation simplicity and unbiased sampling, we use random search with a large evaluation budget of 10 000 candidate evaluations. As the configurations are independently sampled, for evaluating a configuration, we simply blind an initially sampled batch of 10,000 hyperparameter configurations for the hyperparameters not contained in the coalition S by setting their values to the default value. This procedure is fast to compute and reduces the noise potentially occurring through randomly sampling entirely new configurations for every coalition evaluation. After blinding, the surrogate model provided by YAHPO-Gym is then queried for the set of hyperparameter configurations, and the maximum observed performance is returned.

In Figure 7, we show how explanations evolve with higher budgets for simulating a hyperparameter optimization run with random search in combination with a surrogate model. To this end, we investigate explanations obtained through a random search with 10, 100, 1,000, 10,000, and 100,000 hyperparameter configurations sampled during optimization. We find that for low budgets of up to 1,000 samples, explanations are not really stable and change with higher budgets. In particular, we observe higher-order interactions that diminish for higher budgets, reflecting a decreasing uncertainty about the actual interactions. For the higher budgets of 10,000 and 100,000 hyperparameter configurations, the interaction graphs do not change as much, so 10,000 hyperparameter configurations appear to be a reasonable tradeoff between computational complexity and faithfulness of the explanations. Therefore, we chose to conduct our experiments throughout the paper by simulating HPO runs with random search, simulating HPO with a surrogate model and a budget of 10,000 hyperparameter configurations.

B.3. Computing Optimizer Bias

For the experiments considering the HPI game of Data-Specific Optimizer Bias, we designed three HPO methods that focus on different structural parts of the hyperparameter configuration space. For the hyperparameter optimization approach, tuning every hyperparameter individually, when considering a hyperparameter for tuning, we sampled 50 random values for every hyperparameter. For the hyperparameter optimizer focusing on a subset of hyperparameters, we allowed for 50,000 hyperparameter configurations. For the VBO, we employed the considered limited hyperparameter optimizer and a random

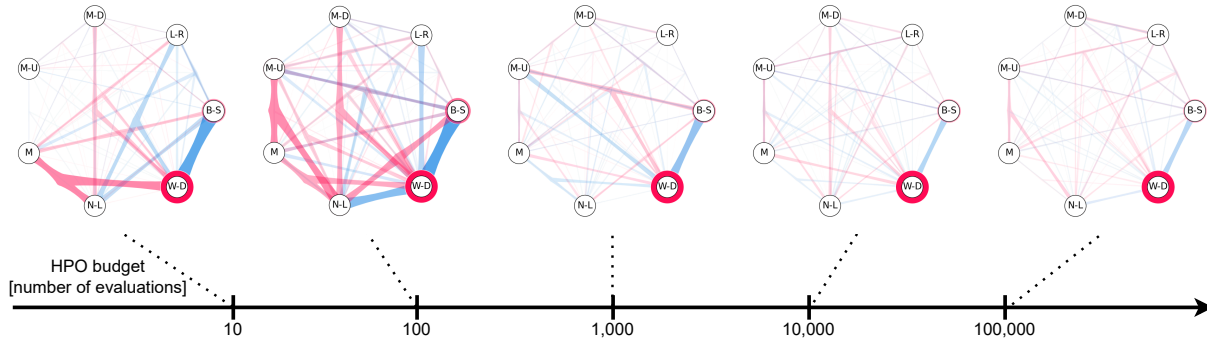


Figure 7. Hyperparameter importance with HyperSHAP, approximating the arg max in Definition 4.3 of the value function via hyperparameter optimization with increasing budgets for dataset ID 7593 of `lcbench`. For tuning, we consider the following hyperparameters of `lcnnet`: learning rate (L-R), batch size (B-S), weight decay (W-D), num layers (N-L), momentum (M), max units (M-U), and max dropout (M-D).

search with a budget of 50,000 evaluations on the full hyperparameter configuration space. We chose larger HPO budgets for these experiments to immediately ensure the built-in deficiencies become apparent and reduce noise effects. However, they might also already be visible with substantially smaller budgets.

B.4. Hardware Usage and Compute Resources

Initial computations for `lcbench` and `rbv2_ranger` have been conducted on consumer hardware, i.e., Dell XPS 15 (Intel i7 13700H, 16GB RAM) and a MacBook Pro (M3 Max - 16C/40G, 128GB RAM). Overall computations took around 10 CPUd, highlighting HYPERSHAP being lightweight when combined with surrogates. In the course of the reviewing process, we re-computed the games for Ablation and Data-Specific Multi-Data Tunability of `lcbench` and `rbv2_ranger` and added PD1 and JAHS-Bench-201. These computations have been conducted on a high-performance computer with nodes equipped with $2 \times$ AMD Milan 7763 (2×64 cores) and 256GiB RAM of which 1 core and 8GB RAM have been allocated to the computations for a single game. While the latter experiments amounted to 10.71 CPU days, in sum, the computations for this paper accumulate roughly 21 CPU days. The average runtimes per benchmark and game are as follows (Table 2):

Table 2. Mean \pm standard deviation of the runtimes on a single CPU per benchmark and game.

Benchmark	$ \Delta $	$ \mathcal{D} $	Runtime Ablation [s]	Runtime Tunability [s]	Runtime Multi-Data Tunability [s]
PD1	4	4	64.9 \pm 16.0	862.4 \pm 13.7	-
JAHS	10	3	123.7 \pm 4.4	30,406.7 \pm 4750.9 (8h26m)	-
LCBench	7	34	4.8 \pm 0.4	357.3 \pm 3.1	10,713.4 (2h58m)
rbv2_ranger	8	119	26.4 \pm 6.8	6,717 \pm 767.3	-

C. Guidance on Interpreting Interaction Visualizations

To visualize and interpret lower-, and higher-order interactions such as SI or MI, we employ the *SI graph visualization* and the *UpSet plot* from `shapiq` (Muschalik et al., 2024a). The SI graph visualization is an extension of the network plot for Shapley interactions (Muschalik et al., 2024b) and can be used to visualize higher order interactions. The UpSet plot (Lex et al., 2014) is a well-established method for visualizing set-based scores, which can also be used for representing higher-order interactions. Figure 8 shows an exemplary SI graph and UpSet plot.

For better readability in terms of the font size, hyperparameter names are abbreviated in the interaction graphs.

Interpretation of the UpSet Plot. An UpSet plot for SIs or MIs shows a selection of high-impact interactions and their scores. The plot is divided into two parts. The upper part shows the interaction values as bars and the lower part shows the considered interactions as a matrix. The first two bars in Figure 8 show the main effects of the O-M and L-I hyperparameters. The third bar shows the negative interaction of both of these features (denoted as the connection between the interactions). A red color denotes a positive score, and a blue color denotes a negative score. The bars and interactions are plotted in descending order according to the absolute value of an interaction (i.e., higher-impact interactions first).

Interpretation of the SI Graph. An SI graph plot in Figure 8 can be interpreted as follows. Each individual player (e.g. hyperparameter) is represented as a node with connecting hyperedges representing the strength and direction of interactions. Akin to the well-established force plots (Lundberg & Lee, 2017), positive interactions are colored in red and negative interactions in blue, respectively. The strength of an interaction is represented by the size and opacity of the hyperedge. To reduce visual clutter, small interactions below a predefined absolute threshold may be omitted from the graph. Notably, first-order interactions (i.e., individual player contributions, or main effects) are represented by the size of the nodes.

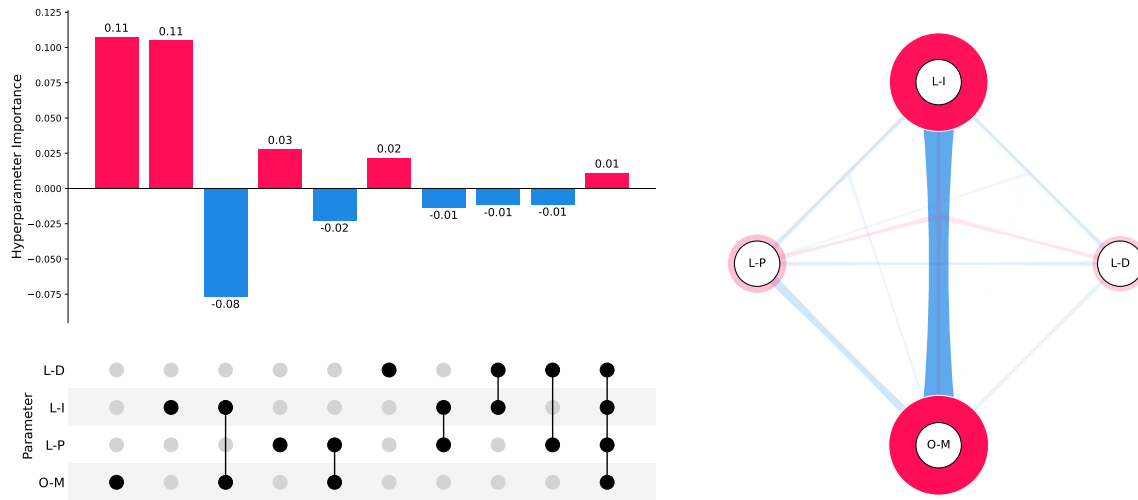


Figure 8. An UpSet plot (left) and a SI graph plot (right) for the Tunability game from Section 5.1.

D. Interaction Quantification in Hyperparameter Optimization

D.1. Measuring the Magnitude of Interactions

In this section, we provide further details for measuring the presence of interactions discussed in Section 5.2. The MIs describe the pure additive effect of a coalition to the payout of the game. They thus serve as an important tool to analyze the interactions present in a game ν . For instance, low-complexity games, where MIs are non-zero only up to coalitions of size k , are typically referred as k -additive games (Grabisch, 2016). In this case, SIs with explanation order k perfectly recover all game values (Bordt & von Luxburg, 2023). In this case, the SIs correspond to the MIs. We thus analyze the absolute values of MIs for varying size of coalitions, i.e., displaying the strata $q(k) := \{|m(S)| : S \subseteq \mathcal{N}, |S| = k\}$ for varying interaction order $k = 1, \dots, n$. Analyzing $q(k)$ indicates, if the game ν has lower- order higher-order interactions present by investigating the magnitudes and distributions in the strata $q(k)$.

D.2. Analyzing Lower-Order Representations of Games

In this section, we provide additional details for the lower-order representations and R^2 scores discussed in Section 5.2. The SV that capture the fair contribution in a game ν of an individual to the joint payout $\nu(\mathcal{N})$. However, the SV $\phi^{\text{SV}}(i)$ is also the solution to a constrained weighted least squares problem (Charnes et al., 1988; Fumagalli et al., 2024b)

$$\phi^{\text{SV}} = \arg \min_{\phi} \sum_{T \subseteq \mathcal{N}} \frac{1}{\binom{n-2}{|T|-1}} \left(\nu(T) - \nu(\emptyset) - \sum_{i \in T} \phi(i) \right)^2 \quad \text{s.t. } \nu(\mathcal{N}) = \nu(\emptyset) + \sum_{i \in \mathcal{N}} \phi(i).$$

In other words, the SV is the best additive approximation of the game ν in terms of this weighted loss constrained on the efficiency axiom. Based on this result, the FSII (Tsai et al., 2023) was introduced as

$$\Phi_k^{\text{FSII}} := \arg \min_{\Phi_k} \sum_{T \subseteq \mathcal{N}} \mu(|T|) \left(\nu(T) - \sum_{S \subseteq T, |S| \leq k} \Phi_k(S) \right)^2 \quad \text{with } \mu(t) := \begin{cases} \mu_{\infty} & \text{if } t \in \{0, n\} \\ \frac{1}{\binom{n-2}{t-1}} & \text{else} \end{cases},$$

where the infinite weights capture the constraints $\nu(\emptyset) = \Phi_k(\emptyset)$ and $\nu(\mathcal{N}) = \sum_{S \subseteq \mathcal{N}} \Phi_k(S)$. Note that Tsai et al. (2023) introduce FSII with a scaled variant of μ that does not affect the solution. The FSII can thus be viewed as the best possible approximation of the game ν using additive components up to order k constrained on the efficiency axiom. It is therefore natural to introduce the *Shapley-weighted faithfulness* as

$$\mathcal{F}(\nu, \Phi_k) := \sum_{T \subseteq \mathcal{N}} \mu(|T|) \left(\nu(T) - \sum_{S \subseteq T, |S| \leq k} \Phi_k(S) \right)^2.$$

Based on this faithfulness measure, the Shapley-weighted R^2 can be computed. More formally, we compute the weighted average and the total sum of squares as

$$\bar{y} := \frac{\sum_{T \subseteq \mathcal{N}} \mu(|T|) \nu(T)}{\sum_{T \subseteq \mathcal{N}} \mu(|T|)} \quad \text{and} \quad \mathcal{F}_{\text{tot}} := \sum_{T \subseteq \mathcal{N}} \mu(|T|) (\nu(T) - \bar{y})^2,$$

which yields the Shapley-weighted R^2 as

$$R^2(k) := R^2(\nu, \Phi_k) := 1 - \frac{\mathcal{F}(\nu, \Phi_k)}{\mathcal{F}_{\text{tot}}}.$$

In our experiments, we rely on FSII, since this interaction index optimizes the faithfulness measure \mathcal{F} by definition. However, k -Shapley Value (k -SII) satisfies a similar faithfulness property (Fumagalli et al., 2024b). Since the FSII is equal to the MIs for $k = n$, we have that $\mathcal{F}(\nu, \Phi_n) = 0$ due to the additive recovery property of the MIs. Hence, $R^2(n) = R^2(\nu, \Phi_n) = 0$ in this case. Clearly, the $R^2(k)$ scores are monotonic increasing in k by definition of FSII. An $R^2(k) \approx 1$ indicates an almost perfect recovery of all game values. In our experiments, we have shown that higher-order interactions are present, but lower-order representations (low k) are mostly sufficient to achieve very high R^2 scores. This indicates that higher-order interactions are present but do not dominate the interaction landscape in our applications. For instance, a single isolated higher-order interaction would yield much lower R^2 scores (Muschalik et al., 2024a).

D.3. Additional Experimental Details

In Section 5.2, we investigate how *faithful* HYPERSHAP explanations capture the interaction structures of the HPO problem. For this we compute Tunability explanations for all four benchmarks, `lcbench`, `rbv2_ranger` PD1, and `JAHS-Bench-201`. Further, we compute Multi-Data Tunability explanations for `lcbench` and `rbv2_ranger` over all instances in the benchmarks. We then compute the MIs for all of these explanations. We compute HYPERSHAP FSII explanations up to the highest order. Then we compute the Shapley-weighted R^2 loss between the explanations and the original game as a measure of *faithfulness*. Figure 9 summarizes the results. The high R^2 score (almost 1.0) for both the Tunability and the Multi-Data Tunability games suggests that most of the explanatory power is captured by interactions up to the third order, confirming prior research that suggests hyperparameter interactions are typically of lower order (Pushak & Hoos, 2020).

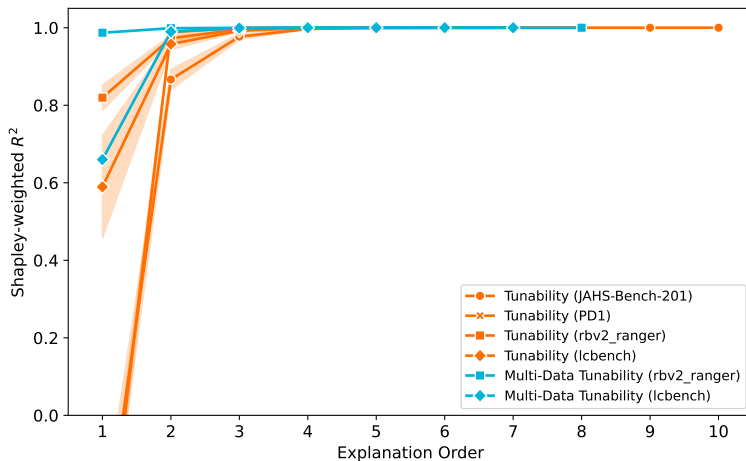


Figure 9. Detailed Reprint of Figure 3 (right). Curves for Multi-Data Tunability contain only one game each. The Tunability games for `lcbench` and `rbv2_ranger` are averaged over 20 randomly selected datasets. The Tunability curves for PD1 and `JAHS-Bench-201` are averaged over all datasets contained in the benchmarks (4 and 3, respectively). The shaded bands correspond to the standard error of the mean (SEM).

E. Additional Empirical Results

This section contains additional experimental results, including more detailed plots and visualizations for the experiments conducted in Section 5.

E.1. Additional Information for the Comparison of Ablation and Tunability

In Section 5.1, we compare the Ablation and the Tunability settings and see that we can derive different interpretations from both explanations into the Hyperparameter optimization. Interpreting the Ablation explanation suggests that only the `lr_initial` (L-I) hyperparameter is important for achieving high performance. However, the Tunability explanation reveals that actually both, the `opt_momentum` (O-M) and `initial_learning_rate` L-I, hyperparameters are useful for tuning. The optimizer needs to decide which hyperparameter to focus on. Figure 10 contains shows the same result as in Figure 2 with more detail.

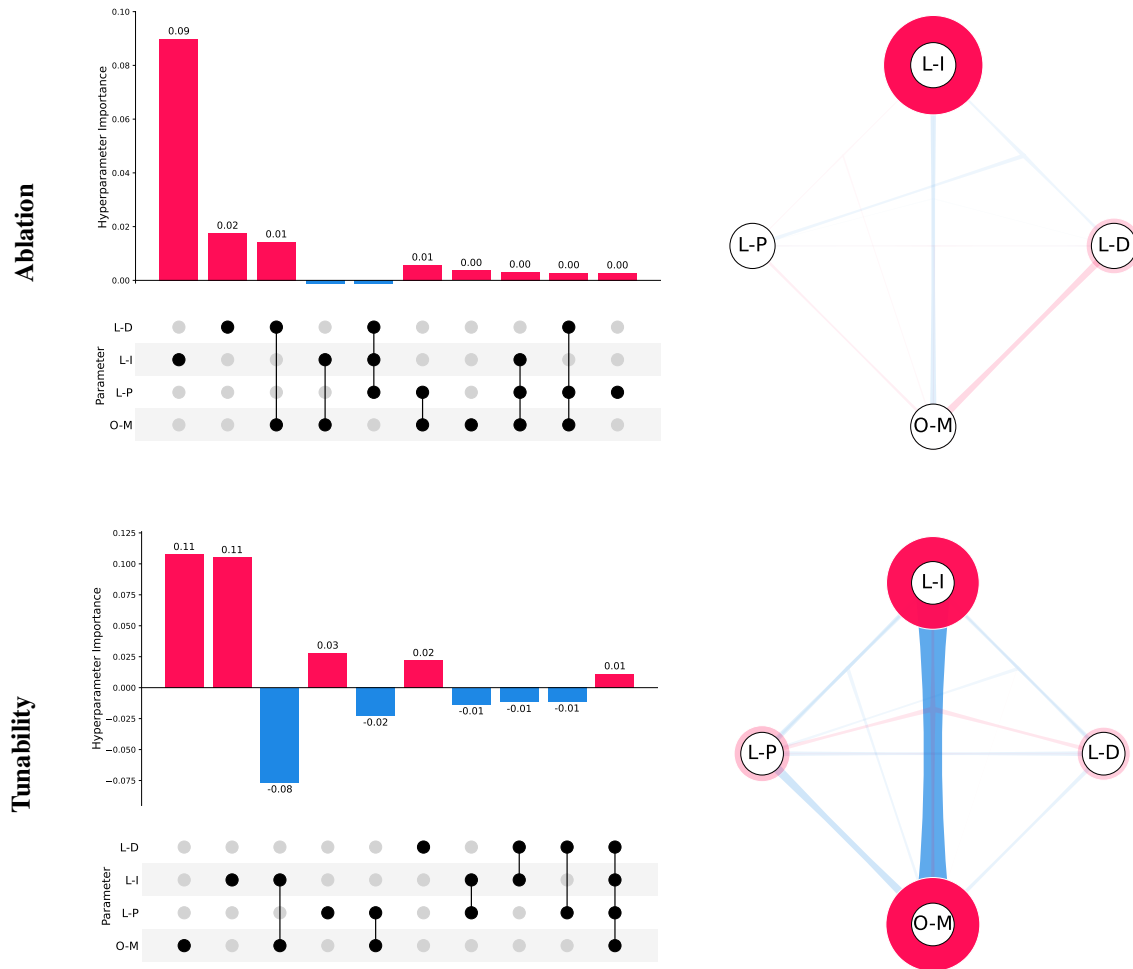


Figure 10. UpSet (left) and SI graph (right) plots for the Ablation (top) and Tunability (bottom) settings described in Section 5.1. The SI graph plots show all interactions and the UpSet plot the ten most impactful interactions.

E.2. Additional Results for Comparison with fANOVA

This section contains additional results for the evaluation of hyperparameter optimization runs restricted to the top-2 important hyperparameters according to fANOVA (Hutter et al., 2014), Sensitivity, and Tunability of HYPERSHAP. Figure 11 shows that selecting and tuning hyperparameters with HYPERSHAP leads to better anytime performance than

with fANOVA or Sensitivity. The suggested top-2 hyperparameters for every method are listed in Table 3. We can observe that overall, although not always perfect, HYPERSHAP suggests a top-2 that yields higher anytime performance, meaning that the hyperparameter optimizer achieves a higher accuracy quicker. However, hyperparameters are suggested with respect to their overall hyperparameter importance, which does not necessarily guarantee better anytime performance as these hyperparameters can be more difficult to tune than others with lower impact. Still, in this case, the lower impact hyperparameters could result in better anytime performance for smaller budgets. We consider an in-depth study of which hyperparameters to suggest for which subsequent HPO task to be an interesting avenue of future work.

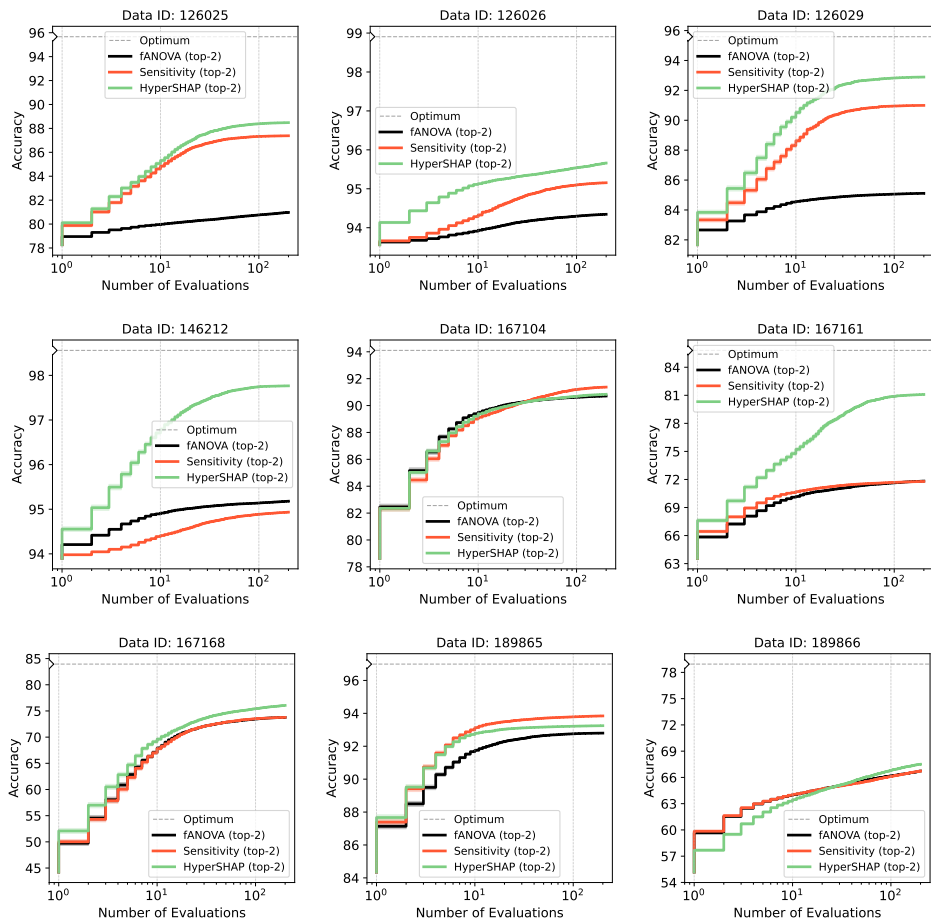


Figure 11. Anytime performance plots showing mean and standard error of the incumbent’s performance, comparing hyperparameter optimization runs restricted to the top-2 important hyperparameters as suggested by fANOVA, the sensitivity game, and the Tunability game of HYPERSHAP.

E.3. Additional Results for Explaining the SMAC Surrogate During Optimization

In Figure 12, in addition to the MI interaction graphs, we summarize explanations with the help of second order FSII, which fairly distributes higher-order interactions to the lower orders, here order one and two. We find that with FSII we can distill the relevant parts of the MIs quite clearly.

E.4. Additional Interaction Visualizations

In Figures 13 to 16, we show more interaction graphs for the different benchmarks we evaluated HYPERSHAP on. This includes PD1 (cf. Figure 13, JAHS-Bench-201 (cf. Figure 14), lcbench (cf. Figure 15), and rbvs_ranger (cf. Figure 16). We find that with HYPERSHAP we can elicit interesting interaction structures for the tuning of transformers and neural architectures in more general. Surprisingly, there can be comparably low interaction between hyperparameters steering the learning behavior and hyperparameters controlling the neural architecture, as seen for CIFAR10. However, for

Table 3. Top-2 Hyperparamters as identified by fANOVA, Sensitivity, and HYPERSHAP

Dataset	fANOVA		Sensitivity		HYPERSHAP	
126025	weight_decay	batch_size	num_layers	learning_rate	num_layers	weight_decay
126026	momentum	learning_rate	learning_rate	num_layers	weight_decay	batch_size
126029	batch_size	momentum	learning_rate	num_layers	num_layers	batch_size
146212	max_dropout	momentum	learning_rate	max_dropout	num_layers	weight_decay
167104	learning_rate	batch_size	learning_rate	num_layers	learning_rate	max_units
167161	learning_rate	max_dropout	learning_rate	batch_size	num_layers	learning_rate
167168	num_layers	learning_rate	learning_rate	num_layers	learning_rate	max_units
189865	num_layers	learning_rate	learning_rate	batch_size	learning_rate	momentum
189866	num_layers	weight_decay	num_layers	weight_decay	weight_decay	max_units

the other two datasets, the higher degree of interaction between the learner’s hyperparameters and those of the architecture better meets intuition and expectation.

In Figure 17, we compare the Sensitivity to the Tunability game for dataset ID 7593 of lcbench on three different levels: Moebius interactions showing all pure effects, Shapley interactions, summarizing higher-order interactions to main effects and interactions of order two and Shapley values representing the entire game solely in terms of main effects. What we can observe is that Tunability and Sensitivity yield quite different explanations as Sensitivity does not blend an optimized hyperparameter configuration with the default hyperparameter configuration for evaluating the value function for a given coalition but takes the variance. Taking the variance apparently results in more pronounced interactivity structures as the performance is no longer contrasted to the default configuration.

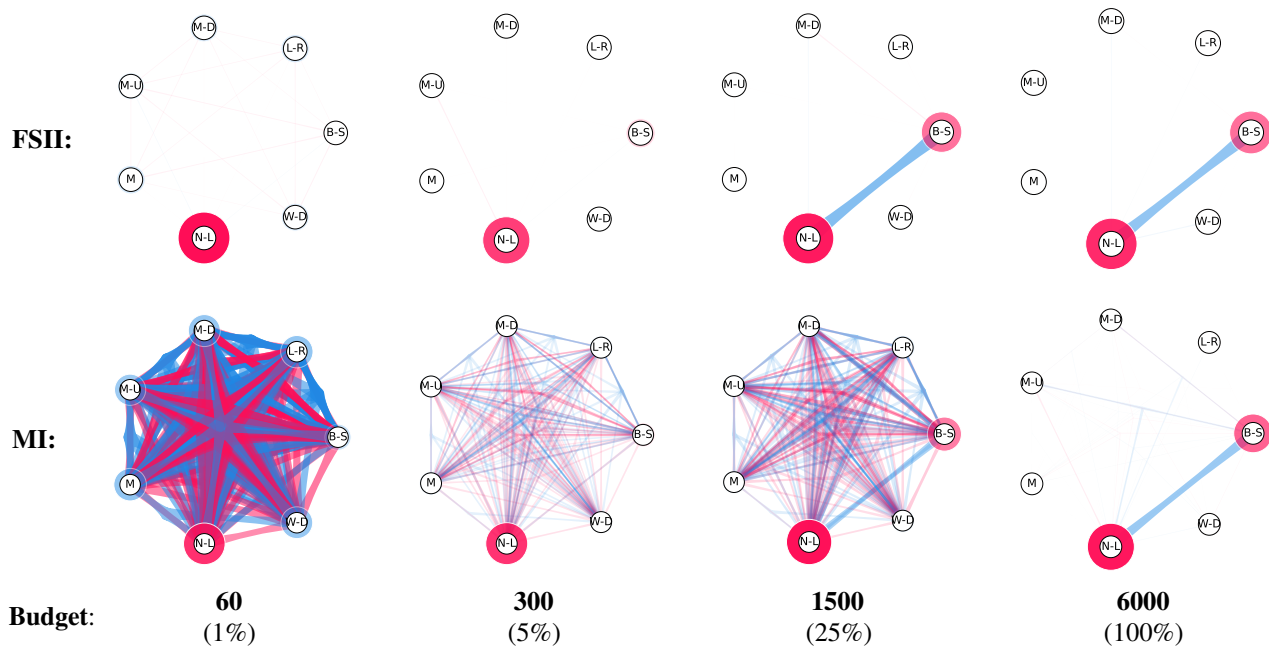


Figure 12. HYPERSHAP Tunability explanations for the surrogate model used in SMAC at different time intervals (1%, 5%, 25%, 100%) of the optimization procedure for dataset 3945 of lcbench (Zimmer et al., 2021). Over time the model becomes less uncertain about which hyperparameters are important to achieve a high predictive performance. Bottom: Interaction graphs for Moebius Interactions (MI) show all pure main effects and interactions. Top: Higher-order interactions are summarized to main effects and second-order interactions, summarizing the game properly already at early stages when the MI still shows a comparably large number of higher-order interactions.

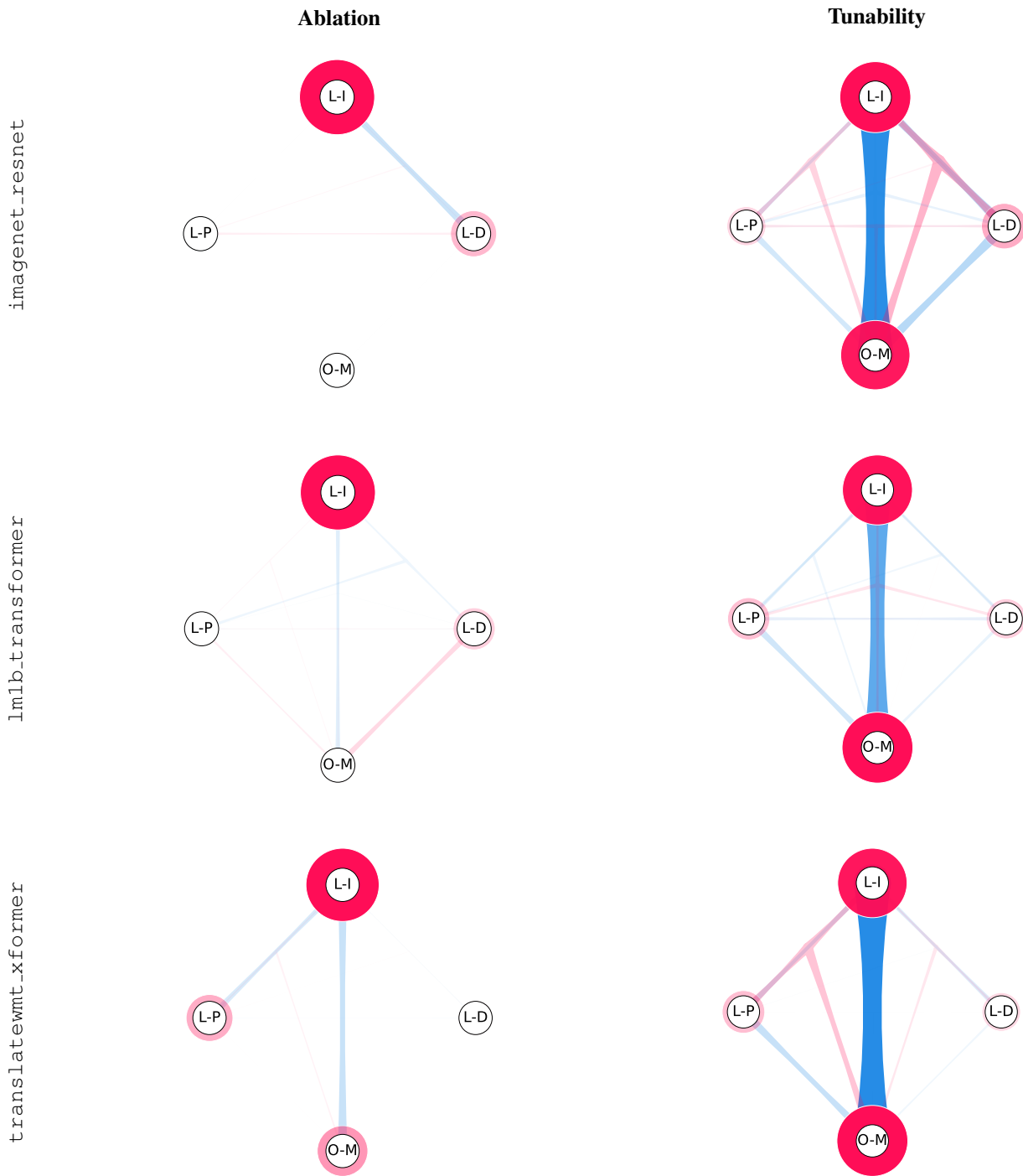


Figure 13. MIs as computed via HYPERSHAP for three different scenarios of PD1, considering hyperparameter optimization for image classifiers and transformers.

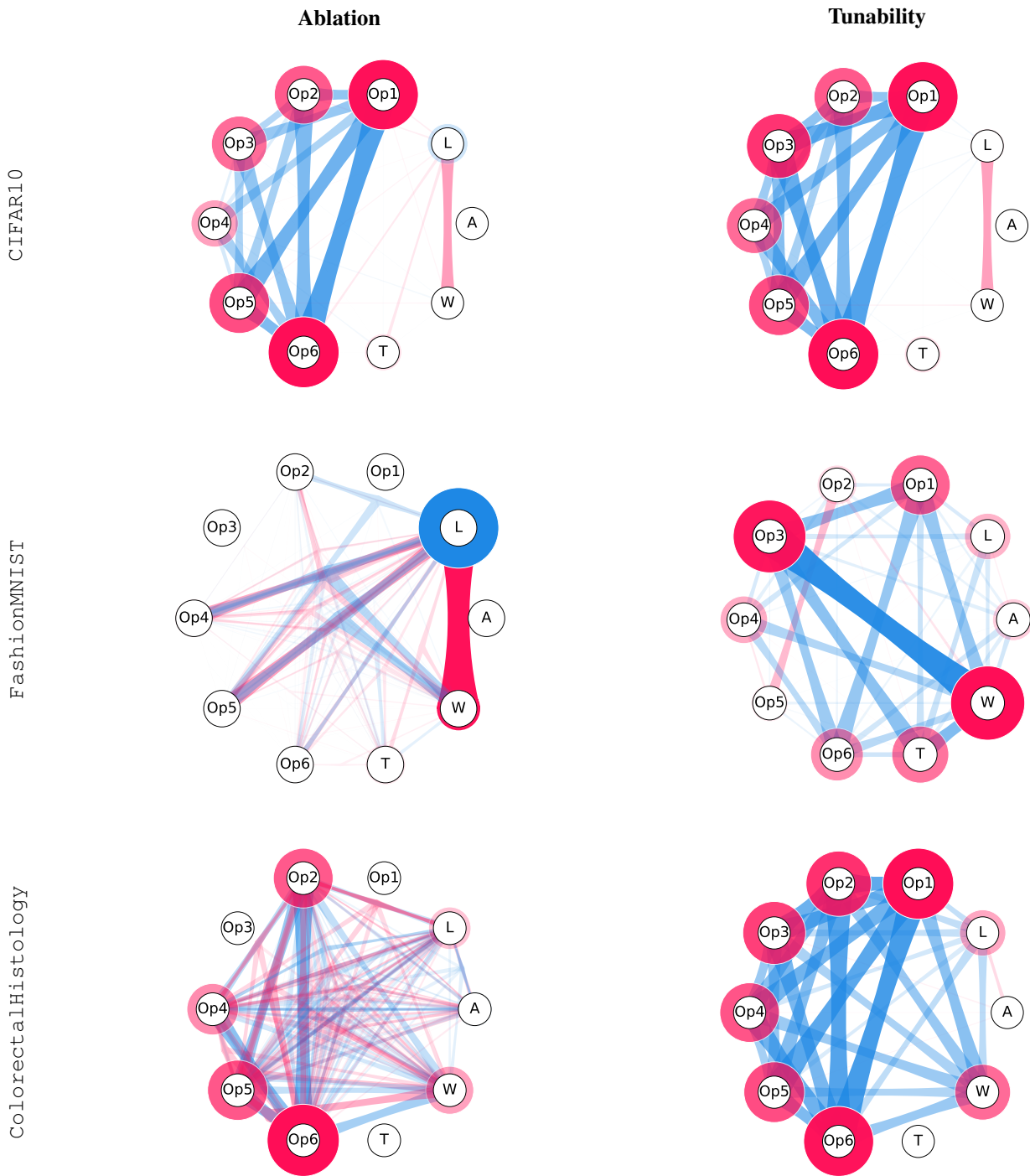


Figure 14. MIs as computed via HYPERSHAP for CIFAR10 (top), FashionMNIST (middle), and ColorectalHistology (bottom) of JAHS-Bench-201.

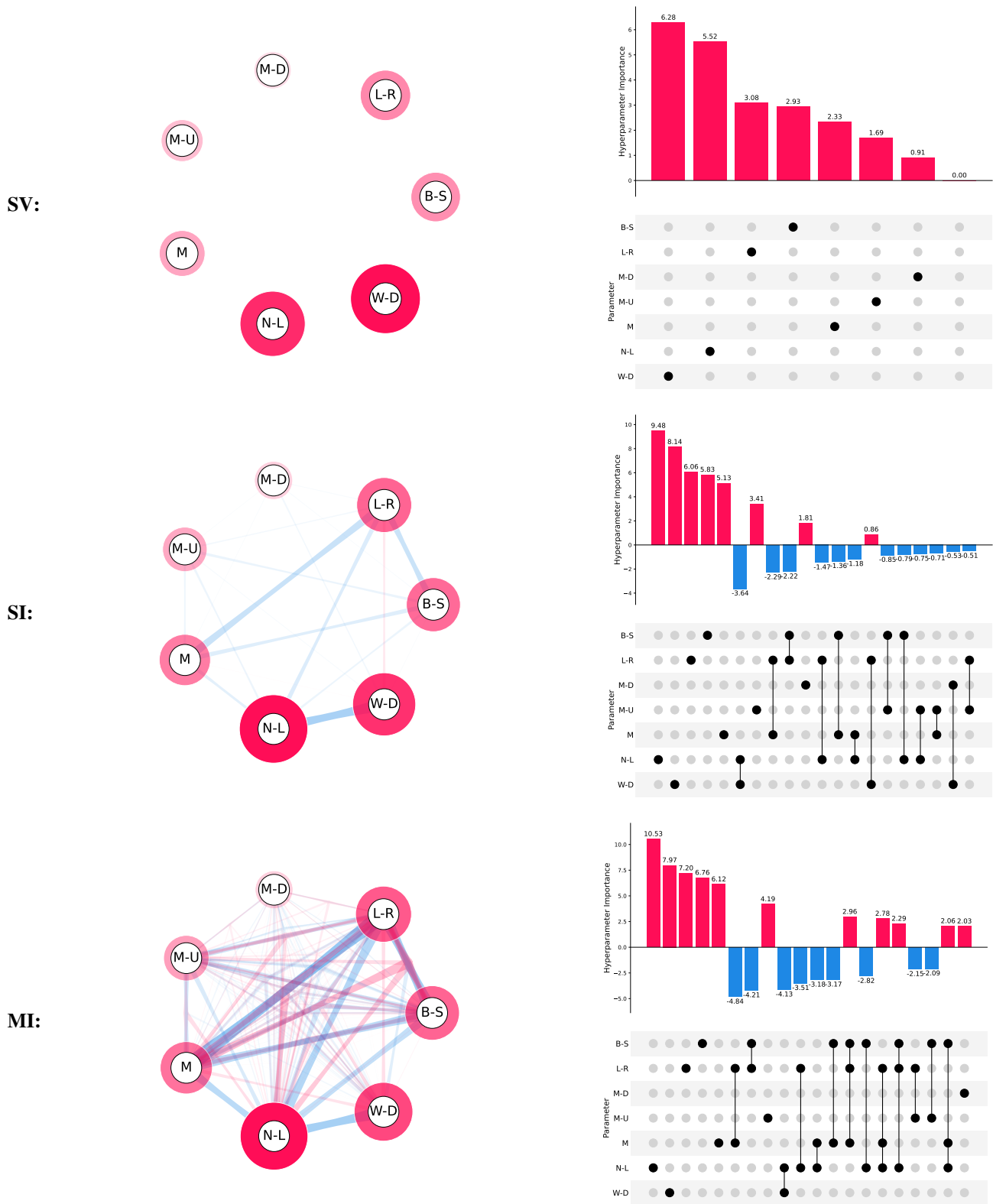


Figure 15. SVs, SIs, and MIs for the Multi-Data Tunability setting on 1cbench. The interactivity in the full decomposition of the MIs is summarized into less complicated explanations by the SVs and SIs. Notably, all SVs are positive.



Figure 16. SVs, SIs, and MIs for the Multi-Data Tunability setting on `rbv2_ranger`. The interactivity in the full decomposition of the MIs is summarized into less complicated explanations by the SVs and SIs. Notably, all SVs are positive.

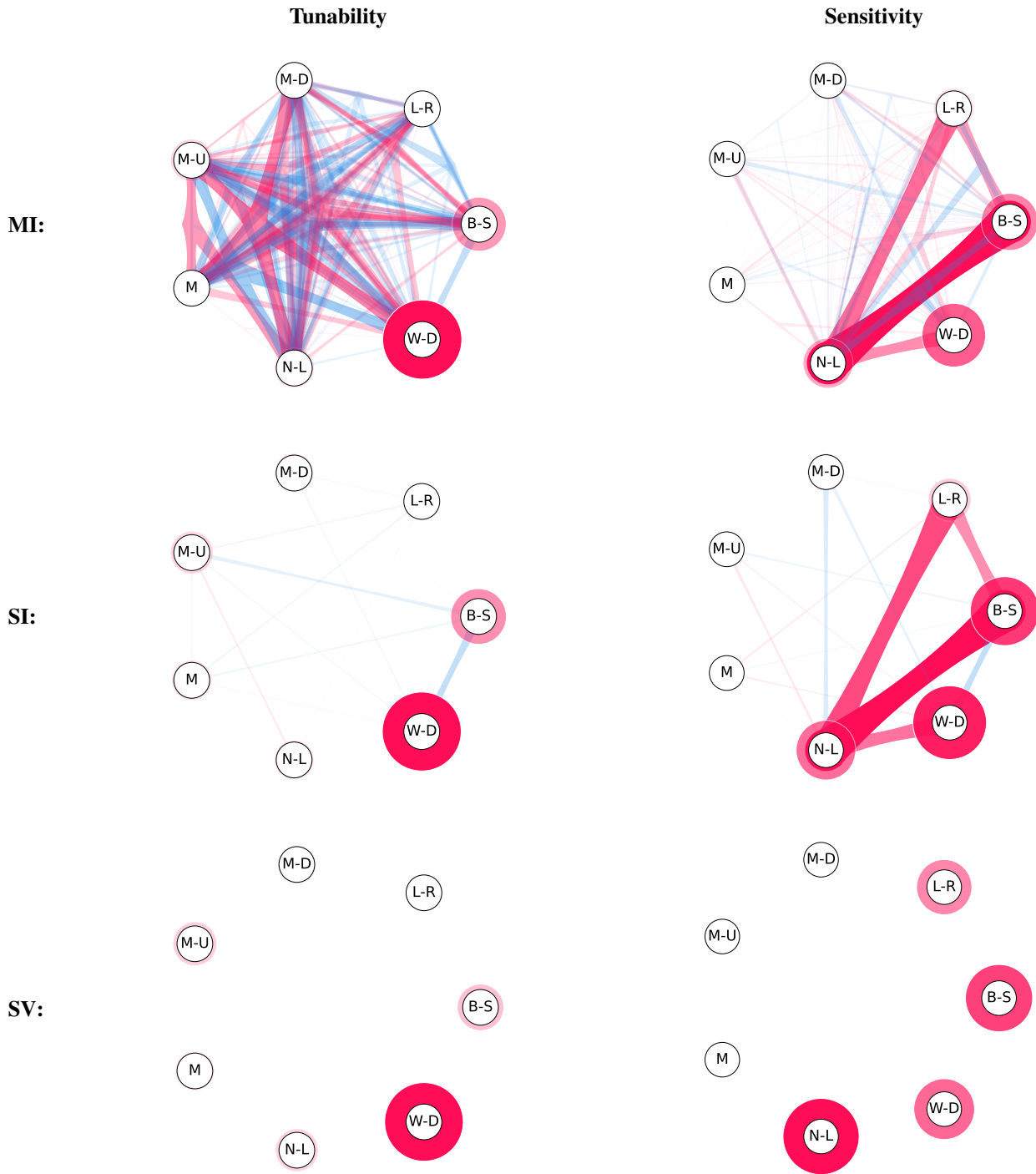


Figure 17. Comparison of Tunability (left) and Sensitivity (right) games as provided via HYPERSHAP. Both variants of measuring HPI provide notably different explanations. Note that also for Sensitivity, HYPERSHAP can be used to compute lower-order explanations summarizing higher-order interactions accordingly.